Title: Improvement of Impact Properties of Tungsten by Potassium Doping

Corresponding Author: Dr. Shuhei Nogami,

Corresponding Author's Institution: Tohoku University

First Author: Shuhei Nogami

Order of Authors: Shuhei Nogami; Shotaro Watanabe; Jens Reiser; Michael Rieth; Sven Sickinger; Akira Hasegawa

Abstract: Low temperature brittleness and high ductile-to-brittle transition temperature (DBTT) are potential drawbacks related to the mechanical properties of tungsten (W) for divertor application in fusion reactors. To improve the mechanical properties of W, potassium (K) doping has been applied as a dispersion-strengthening method. In this paper, the effects of K-doping on the Charpy impact properties of W plate fabricated by powder metallurgy and hot rolling in the as-received condition were investigated. In addition, the correlation among the impact properties, tensile properties, and grain structure and the advantages of K-doped W for divertor application of fusion reactor were discussed.

Research Data Related to this Submission

There are no linked research data sets for this submission. The following reason is given:
The authors do not have permission to share data

Improvement of Impact Properties of Tungsten by Potassium Doping

Shuhei Nogami[1], Shotaro Watanabe[2], Jens Reiser[3], Michael Rieth[4], Sven Sickinger[5],

Akira Hasegawa[6]

[1] Department of Quantum Science and Energy Engineering, Graduate School of Engineering, Tohoku University, 6-6-01-2, Aramaki-aza-Aoba, Aoba-ku, Sendai 980-8579, Japan, shuhei.nogami@qse.tohoku.ac.jp

[2] Department of Quantum Science and Energy Engineering, Graduate School of Engineering, Tohoku University, 6-6-01-2, Aramaki-aza-Aoba, Aoba-ku, Sendai 980-8579, Japan, shotaro.watanabe.s5@dc.tohoku.ac.jp

[3] Institute for Applied Materials, Karlsruhe Institute of Technology, Hermann-von-Helmholtz-Platz 1, 76344 Eggenstein-Leopoldshafen, Germany, jens.reiser@kit.edu

[4] Institute for Applied Materials, Karlsruhe Institute of Technology, Hermann-von-Helmholtz-Platz 1, 76344 Eggenstein-Leopoldshafen, Germany, michael.rieth@kit.edu

[5] Institute for Applied Materials, Karlsruhe Institute of Technology, Hermann-von-Helmholtz-Platz 1, 76344 Eggenstein-Leopoldshafen, Germany, sven.sickinger@kit.edu

[6] Department of Quantum Science and Energy Engineering, Graduate School of Engineering, Tohoku University, 6-6-01-2, Aramaki-aza-Aoba, Aoba-ku, Sendai 980-8579, Japan, akira.hasegawa@qse.tohoku.ac.jp

[7]

Corresponding Author

Name   Shuhei Nogami

Postal address   Department of Quantum Science and Energy Engineering, Graduate School

of Engineering, Tohoku University, 6-6-01-2, Aramaki-aza-Aoba, Aoba-ku,

Sendai 980-8579, Japan

Telephone   +81-22-795-7923

Fax number   +81-22-795-7924

E-mail address   shuhei.nogami@qse.tohoku.ac.jp

RESPONSES TO THE REVIEWERS

REVIEWER #1:

The details necessary for judgement of material properties is yet to be added. This relates to the details of sample manufacturing. Presently, very scarce information is given. Important details are:

1. Purity of the source material
2. Details on HIPing
    *   Temperature
    *   Duration
    *   Pressure

Was inert atmosphere used or was it vacuum sintering?

[Response]

Thank you for your comment. First of all, our materials were fabricated not by a HIPing but by a hot-rolling. We have added the temperature condition of cold isostatic pressing, sintering, and hot rolling as important information of fabrication conditions. We have also added the content of interstitial impurities (C, O, and N) in three materials and content of K in KW-7.

Highlights

(1) Effects of K-doping on the Charpy impact properties of hot-rolled W plate were investigated.

(2) K-doped W showed increase in USE and decrease in DBTT compared to pure W with the same deformation ratio.

(3) DBTT and USE of W materials from different production routes could be predicted using Hall-Petch type relations regardless of the K-doping.

(4) K-doping simultaneously induced grain refining, suppression of recrystallization, increases in strength, ductility, and impact properties.

Improvement of Impact Properties of Tungsten by Potassium Doping

Shuhei Nogami[1], Shotaro Watanabe[2], Jens Reiser[3], Michael Rieth[4], Sven Sickinger[5],

Akira Hasegawa[6]

[1]   Department of Quantum Science and Energy Engineering, Graduate School of Engineering, Tohoku University, 6-6-01-2, Aramaki-aza-Aoba, Aoba-ku, Sendai 980-8579, Japan, shuhei.nogami@qse.tohoku.ac.jp

[2]   Department of Quantum Science and Energy Engineering, Graduate School of Engineering, Tohoku University, 6-6-01-2, Aramaki-aza-Aoba, Aoba-ku, Sendai 980-8579, Japan, shotaro.watanabe.s5@dc.tohoku.ac.jp

[3]   Institute   for   Applied   Materials,   Karlsruhe   Institute   of   Technology, Hermann-von-Helmholtz-Platz   1,   76344   Eggenstein-Leopoldshafen,   Germany, jens.reiser@kit.edu

[4]   Institute   for   Applied   Materials,   Karlsruhe   Institute   of   Technology, Hermann-von-Helmholtz-Platz   1,   76344   Eggenstein-Leopoldshafen,   Germany, michael.rieth@kit.edu

[5]   Institute   for   Applied   Materials,   Karlsruhe   Institute   of   Technology, Hermann-von-Helmholtz-Platz   1,   76344   Eggenstein-Leopoldshafen,   Germany, sven.sickinger@kit.edu

[6]   Department of Quantum Science and Energy Engineering, Graduate School of Engineering, Tohoku University, 6-6-01-2, Aramaki-aza-Aoba, Aoba-ku, Sendai 980-8579, Japan, akira.hasegawa@qse.tohoku.ac.jp

Corresponding Author

Name   Shuhei Nogami

Postal address   Department of Quantum Science and Energy Engineering, Graduate School

                        of Engineering, Tohoku University, 6-6-01-2, Aramaki-aza-Aoba, Aoba-ku,

                        Sendai 980-8579, Japan

Telephone   +81-22-795-7923

Fax number   +81-22-795-7924

E-mail address   shuhei.nogami@qse.tohoku.ac.jp

Improvement of Impact Properties of Tungsten by Potassium Doping

Shuhei Nogami[1], Shotaro Watanabe[1], Jens Reiser[2], Michael Rieth[2], Sven Sickinger[2],

Akira Hasegawa[1]

[1] Department of Quantum Science and Energy Engineering, Graduate School of

Engineering, Tohoku University, 6-6-01-2, Aramaki-aza-Aoba, Aoba-ku, Sendai

980-8579, Japan

[2] Institute for Applied Materials, Karlsruhe Institute of Technology,

Hermann-von-Helmholtz-Platz 1, 76344 Eggenstein-Leopoldshafen, Germany

Abstract

Low temperature brittleness and high ductile-to-brittle transition temperature

(DBTT) are potential drawbacks related to the mechanical properties of tungsten (W) for

divertor application in fusion reactors. To improve the mechanical properties of W, potassium

(K) doping has been applied as a dispersion-strengthening method. In this paper, the effects

of K-doping on the Charpy impact properties of W plate fabricated by powder metallurgy and

hot rolling in the as-received condition were investigated. In addition, the correlation among

the impact properties, tensile properties, and grain structure and the advantages of K-doped

W for divertor application of fusion reactor were discussed.

Keywords:

Tungsten, Charpy impact property, Dispersion strengthening, Potassium doping, Grain

refining, Hall-Petch law

1. Introduction

Tungsten (W) is a promising plasma-facing material for fusion reactor divertors because of its high melting point, high thermal conductivity, low tritium retention, and low sputtering rate [1]. However, there remain some drawbacks related to the mechanical properties of W materials, e.g., low temperature brittleness, high ductile-to-brittle transition temperature (DBTT) [2–10], recrystallization-induced embrittlement [11–14], and neutron-irradiation-induced embrittlement [15–18]. These issues will restrict the operating temperature window of fusion reactor divertors using W as a plasma-facing material.

To suppress the brittleness of W, various approaches including alloying and microstructural control have been explored. Grain refining [19], work hardening [20], solid solution alloying [21, 22], and dispersion strengthening [22, 23] are known as conventional methods for improving the mechanical properties and suppressing the recrystallization of W materials. Potassium (K) doping is a dispersion-strengthening method for W materials and has been historically used for W filaments etc. [23–26]. K-doped W contains nano-bubbles including K atoms (on the order of ppm), which are mainly dispersed at the grain boundaries [23]. K bubbles are produced during sintering by the volatilization of K, which is added to the raw material powder. Because K bubbles can hinder the motion of grain boundaries and dislocations, they lead to strengthening at a high temperature and suppression of recrystallization [24, 26]. In addition, K-doping can produce finer grains compared to pure W because K bubbles inhibit grain boundary migration in general [26]. This grain refining also leads to strengthening, which can be explained in general by the Hall–Petch law [27, 28]. Improvement in the mechanical properties by grain refining have been observed for most metals including W [29, 30]. Moreover, it is expected that neutron-irradiation-induced embrittlement can be suppressed in K-doped W compared to pure W because it contains a large number of grain boundaries that act as sinks for defects formed by the neutron

irradiation.

Because most applications of K-doping have been for filaments etc. [23–26], limited data are available for bulk K-doped W materials, which can be applied to the plasma-facing material of a fusion reactor divertor. Most bulk K-doped W materials, which are expected to be applied to plasma-facing materials, showed improvements in their thermo-mechanical properties compared to pure W, including the recrystallization temperature, tensile properties, low cycle fatigue life, and thermal shock resistance [31–38]. However, the K-doping showed no significant positive effects on the impact properties below 1000 °C in the case of hot-rolled W plates [39, 40]. In the case of swaged W rods, K-doping induced decreases in the upper shelf energies (USE) above 800 °C in comparison with pure W, although it induced a decrease of 50–100 °C in the DBTT [39, 40]. In principle, the effects of K-doping on the mechanical properties were expected especially at a higher temperature, e.g., above half of the melting temperature inducing creep deformation. For W materials, the method of K-doping was originally developed to suppress creep deformation caused by grain boundary sliding. Therefore, no significant positive effects of K-doping on the impact properties could be found below 1000 °C.

On the other hand, grain refining, which can generally improve the strength, was achieved by K-doping. In our previous studies [33–38], K-doped W plates and rods showed an improvement in the tensile strength below 1000 °C in comparison with that of pure W materials, which could be attributed to K-doping. As mentioned before, these improvements were considered to be mostly caused by grain refining due to K-doping and by the dispersion of K bubbles, which can hinder the motion of grain boundaries and dislocations. The impact properties are simultaneously influenced by the strength and ductility. Therefore, it is necessary to further investigate the effects of K-doping on the impact properties of W materials from strength, ductility, and microstructural viewpoints.

The objectives of the present study are to investigate the grain structure, tensile properties, and Charpy impact properties of pure W and K-doped W plates and to discuss the effects of K-doping on the impact properties observed from these experiments. It is well known that rolled W materials show a microstructural anisotropy, which is strongly dependent on the fabrication conditions. The materials used in the present study also have a microstructural anisotropy, as discussed in section 3.1, which will induce anisotropies of thermo-mechanical properties. A few published papers have already reported anisotropy in the tensile and Charpy impact properties of some materials used in the present study [33, 39]. However, the tensile and Charpy impact properties along the selected direction were evaluated in the present study to evaluate the effects of K-doping. The effect of the microstructural anisotropy will be discussed in future papers.

2. Experimental

2.1 Materials and grain structure evaluation

A pure W plate with a thickness of 4 mm (PW-4), a pure W plate with a thickness of 7 mm (PW-7), and a K-doped W plate with a thickness of 7 mm (KW-7) were examined in the present study, which were fabricated by powder metallurgy (cold isostatic pressing at room temperature and sintering at 1800–2200 °C) and hot rolling at 1400–1600 °C followed by a final heat treatment at approximately 900 °C for stress relief. The concentration of carbon (C), oxygen (O), and nitrogen (N) as interstitial impurities in all three materials were approximately 10 ppm, less than 10 ppm, and less than 10 ppm, respectively. The concentration of K in KW-7 were approximately 30 ppm. The thickness mentioned above were those obtained directly after rolling. The reduction ratio (deformation ratio) for the hot-rolling of PW-4 was approximately 10% higher than those of PW-7 and KW-7. All three materials were prepared in the as-received (hot-rolled and stress-relieved) condition.

The purposes of utilizing these three materials were not only to evaluate the direct availability of these materials as the plasma-facing material of fusion reactor divertors but to evaluate the effectiveness of grain refining and K-doping from the viewpoints of the thermo-mechanical properties of W materials for divertor applications. Although it is possible that the thicknesses of 4 mm and 7 mm are not sufficient for divertor fabrication (e.g., the thickness of around 12 mm for ITER monoblock divertor targets), the effect of grain refining due to the increase in the deformation ratio and the effect of K-doping, which includes the dispersion of K-bubbles and grain refining with no increase in the deformation ratio, could be estimated by comparisons between PW-4 and PW-7 and between PW-7 and KW-7, respectively. Because a material with a sufficient volume for divertor application and the same microstructure as the materials used in the present study could be obtained by using appropriate fabrication facilities (facilities for sintering, rolling, etc.), the knowledge obtained in the present study will be available for the future development of fusion reactor divertors using W materials.

To observe the grain structure and measure the grain size, mechanical polishing and electrolytic polishing using a solution of sodium hydroxide and potassium ferricyanide were conducted on the "L × T," "T × S," and "S × L" surfaces. The orientations of the L, T, and S directions are shown in Fig. 1. The L direction corresponds to the rolling direction of the plate. The grain sizes were measured based on the ASTM E112-85 standard [41] with metallographic images after polishing.

2.2 Tensile test

To investigate the tensile properties (ultimate tensile strength, 0.2% yield stress, total elongation, and reduction in area) of PW-4, PW-7, and KW-7, tensile tests along the L direction were carried out at various temperatures. Some tensile tests were performed in

previous studies and data have already been published [33, 37, 38]. Flat-plate specimens were used for the tensile tests, as shown in Fig. 1 (a) as the SS-J tensile specimen. The dimensions of the specimen gauge section were 5 mm × 1.2 mm × 1.0 mm. The loading axis of the specimens was aligned along the L direction (rolling direction) of the materials. The tensile tests were carried out at temperatures ranging from room temperature to 1300 °C in vacuum at a pressure of approximately 10^{-3} Pa at a strain rate of 1×10^{-3} s^{-1}. Specimens were held for 1 h at each test temperature before tensile tests. The number of tests at each temperature was one or two. The ultimate tensile strength, 0.2% yield stress, total elongation, and reduction in area were evaluated using the average value if the number of tests was two. The ruptured specimens were observed by a scanning electron microscope (SEM) to evaluate the reduction in area.

To investigate the effect of the strain rate on the fracture manner of PW-7 and KW-7, tensile tests along the S direction were carried out at various strain rates. Flat-plate specimens were used for the tensile tests, as shown in Fig. 1 (b) as the VS-T tensile specimen. The dimensions of the specimen gauge section were 1.05 mm × 1.2 mm × 1.0 mm. The loading axis of the specimen was aligned along the S direction of the materials. Tensile tests were carried out at room temperature and 700 °C in vacuum at a pressure of approximately 10^{-3} Pa at strain rates of 1×10^{-3} s^{-1} and 1×10^{-1} s^{-1}. Specimens were held for 1 h before tensile tests at 700 °C. The number of tests at each temperature was one. The ruptured specimens were observed by an SEM to evaluate the fracture manner.

2.3 Charpy impact test

The specimens and methods for instrumented Charpy impact testing were based on the EU standard DIN EN ISO 14556:2017-05 [42]. KLST Charpy V-notched specimens with a length of 27 mm, a width of 3 mm, and a thickness of 4 mm were utilized, as shown in Fig.

1 (c). The depth and root radius of the notch were 1 mm and 0.1 mm, respectively. The span of the lower-die of this testing machine was 22 mm for all tests. Charpy impact tests along the L-S direction were carried out at temperatures ranging from 300 °C to 1000 °C in vacuum at a pressure of approximately 10^{-2} Pa using a Charpy impact testing machine with a high temperature vacuum furnace at the Institute of Applied Materials (IAM), Karlsruhe Institute of Technology (KIT), Germany [39]. The nomenclature of the L-S direction is shown in Fig. 1 (d). The first letter (L) indicates the direction perpendicular to the expected crack plane while the second letter (S) stands for the expected direction of crack growth. Specimens were held for 1 h at each test temperature before impact tests. The number of tests at each temperature was one, except the test of KW-7 at 600 °C (The number of tests was two.). The ruptured specimens were observed by an SEM to evaluate the fracture manner. Some Charpy impact tests were performed in previous studies and data have already been published [39, 40, 43–47].

3.   Results and Discussion

3.1 Grain structure

Fig. 2 shows images of the grain structures of PW-4, PW-7 [47], and KW-7, which were obtained by optical microscope observations and electron backscatter diffraction (EBSD) analyses. All three materials showed grains with a "pancake" shape, which is particular to W materials fabricated by powder metallurgy and hot rolling.

Fig. 3 shows the average grain sizes along the L, T, and S directions (d_L, d_T, and d_S, respectively) of PW-4 [47], PW-7 [47], and KW-7. The orientations of these directions are shown in Figs. 1 and 2. The L direction corresponds to the rolling direction of the plate. The grain sizes of PW-4 were smaller than those of PW-7 regardless of the direction. Because the deformation ratio for the hot-rolling of PW-4 was approximately 10% higher than that of

PW-7, the grains of PW-4 could be refined to a much greater degree than those of PW-7.

The grain sizes along all three directions of KW-7 were smaller than those of PW-7. As mentioned in section 1, K-doping can induce the grain refining of W in general, even if the deformation ratio is the same, because the K-bubbles dispersed in the grain boundaries could hinder the motion of grain boundaries and dislocations [26]. Because the deformation ratio for the hot-rolling of KW-7 was the same as that of PW-7, smaller grains could be achieved in KW-7 compared to those in PW-7 by K-doping.

3.2 Tensile properties

3.2.1 Strength

The test temperature dependences of the tensile properties (ultimate tensile strength, 0.2% yield stress, total elongation, and reduction in area) at a strain rate of 1×10^{-3} s^{-1} along the L direction of PW-4, PW-7 [33, 37, 38], and KW-7 [33, 37, 38] are shown in Fig. 4. As shown in Figs. 4 (a) and (b), the ultimate tensile strength and 0.2% yield stress of PW-4 were higher than those of PW-7. It is well known that grain refining can improve the strength of most metals including W [29, 30], even if their major chemical compositions are the same, which can be explained in general by the Hall–Petch law [27, 28]. Therefore, the strengthening in PW-4 could be attributed to grain refining caused by the increase in the deformation ratio for the hot-rolling, as mentioned in the last section.

KW-7 showed a higher ultimate tensile strength and 0.2% yield stress compared to those of PW-7, which were similar to those of PW-4. As mentioned in the last section, grain refining could occur by K-doping compared to pure W despite no change in the deformation ratio for the hot-rolling. Therefore, it was possible that K-doping was one method for strengthening W materials based on the grain refining effect with no increase in the deformation ratio. The effect of the dispersion of K bubbles on the tensile strength was

uncertain from the results of the present study.

3.2.2 Ductility

As shown in Figs. 4 (c) and (d), the total elongation and reduction in area of PW-4 were lower than those of PW-7. Because most of metals simultaneously show an increase in strength and a decrease in ductility in general, these results were plausible.

There were no significant differences in the total elongation and reduction in area for PW-7 and KW-7 from 300 °C to 900 °C. In contrast, the total elongation and reduction in area of KW-7 were higher than those of PW-7 at test temperatures below 300 °C. Although the total elongation and reduction in area of PW-7 were zero below 100 °C, those of KW-7 were not zero above room temperature. Therefore, it was possible that K-doping was one method for improving the ductility, especially in the low temperature range. At a test temperature of 1300 °C, the total elongation and reduction in area of PW-7 and KW-7 were relatively large compared to those at the other test temperatures. According to the report by Sheng *et al*. [32], recrystallized W materials showed no visible dislocation lines and a relatively large elongation in a tensile test, while the as-received materials showed dislocation lines and a relatively small elongation. As described in section 3.4 in detail, recrystallization started in the ranges of 1100–1200 °C in PW-7 and 1200–1300 °C in KW-7 [48]. Therefore, relatively large values of the total elongation and reduction in area could be attributed to the recrystallized grains with a very low density of dislocations caused by annealing.

3.3 Charpy impact properties

3.3.1 DBTT and USE

The test temperature dependences of absorbed energy from Charpy impact tests of KLST specimens of PW-4, PW-7, and KW-7 along the L-S direction are shown in Fig. 5. The

data of PW-4 and PW-7 were taken from our previous studies [39, 40, 43–45, 47]. This figure also includes the data of a pure W round-blank with a diameter of 175 mm and a thickness of 29 mm (PW-29) fabricated by powder metallurgy and forging [45, 46]. The DBTT and USE varied widely among the materials. The DBTTs of PW-4, PW-7, PW-29, and KW-7 were approximately 450, 550, 710, and 350 °C, respectively. The USEs of PW-4, PW-7, PW-29, and KW-7, which were the average values of the absorbed energy from the DBTT to 1100 °C, were approximately 6.8, 5.5, 4.0, and 7.6 J, respectively. As shown in Fig. 6, a linear relation between the DBTT and the USE was obtained regardless of the production methods, histories, and K-doping. In this figure, the error bars of the USE indicate the difference of the maximum and minimum absorbed energies from the USE. These wide-ranged impact properties might be attributed to the individual particular microstructure dependent on the fabrication methods, histories, and K-doping. According to our previous study [47], the facts that the impact properties of PW-4 were better than those of PW-7 and that the impact properties of PW-7 were better than those of PW-29 can be explained by the strengthening due to grain refining, which was caused by the increase in the deformation ratio. Compared to these three pure W materials, KW-7 showed superior impact properties. Although the superior performance of KW-7 could be also related to the grain refining, it was produced not only by the increase in the deformation ratio but by the K-doping. The details of the effects of K-doping (grain refining, K bubbles, etc.) on the impact properties are discussed in section 3.3.5.

3.3.2 Fracture manner

The appearances of the KLST specimens of PW-7 and KW-7 after the impact tests are shown in Figs. 7 (a) and (b), respectively. Below the DBTT, brittle fracture and a mixture of brittle and delamination fractures were observed at test temperatures of 400 °C for PW-7

and 300 °C for KW-7. The fracture surfaces of PW-7 and KW-7 showed cleavage and intergranular at sub-grain boundaries, respectively, as shown in Figs. 8 (b) and (d). According to the report by Curry and Knott [49], the cleavage fracture stress of several steels could increase with refining the grain size. Therefore, cleavage fracture was suppressed in KW-7 because of grain refining compared to PW-7. In contrast, as shown in Figs. 7 (a) and (b), delamination fracture was observed in both materials at all test temperatures above the DBTT and below 1000 °C. The direction of delamination was parallel to the rolling direction (L direction). These fracture manners below and above the DBTT were similar to those observed for PW-4 [39, 40, 43–45] and PW-29 [45, 46]. As shown in Figs. 8 (a) and (c), the fracture surfaces for delamination showed intergranular at sub-grain boundaries, which were observed in both materials at all test temperatures above the DBTT and below 1000 °C.

3.3.3 Effect of strain rate

In general, the strain rate applied during a Charpy impact test is higher than that of ordinary static mechanical tests. To investigate the effect of the strain rate on the fracture manner of PW-7 and KW-7, tensile tests were carried out along the S direction using VS-T specimens at room temperature and 700 °C at strain rates of 1×10^{-3} and 1×10^{-1} s^{-1}. The ultimate tensile strength, 0.2% yield stress, total elongation, reduction in area, and fracture manner from these tensile tests are summarized in Table 1. The fracture surfaces observed using an SEM are also shown in Fig. 9.

At a lower strain rate (1×10^{-3} s^{-1}, Figs. 9 (a), (b), (e), and (f)), most of the specimens showed intergranular fracture at sub-grain boundaries, except PW-7 at room temperature, which showed cleavage fracture, as shown in Fig. 9 (a). As described in the last section, the cleavage fracture stress could increase with refining the grain size [49]. Because larger grains were observed in PW-7 compared to KW-7, the cleavage fracture stress of PW-7

could be lower than that of KW-7. Therefore, it is possible that PW-7 and KW-7 showed different fracture manner at room temperature because of the difference in their cleavage fracture stresses. On the other hand, at a higher strain rate condition (1×10^{-1} s^{-1}, Figs. 9 (c), (d), (g), and (h)), no difference in the fracture manner was observed for PW-7 and KW-7. Both showed intergranular fracture at sub-grain boundaries regardless of the test temperature. In contrast, the Charpy impact tests, which could induce loading with a relatively high strain rate in materials, showed a difference in the fracture manner between them at temperatures below the DBTT. PW-7 and KW-7 showed cleavage fracture and intergranular fracture at sub-grain boundaries, respectively. Therefore, the results of the tensile tests along the S direction at room temperature and 700 °C at strain rates of 1×10^{-3} s^{-1} and 1×10^{-1} s^{-1} could not support the differences in the fracture manner from the Charpy impact tests. Further investigation of the effect of strain rate is planned as future work.

3.3.4 Effect of strength and ductility

To discuss the effects of the strength and ductility on the Charpy impact properties at test temperatures above the DBTT, the correlation between the absorbed energy from the Charpy impact tests described in this section and the tensile properties described in section 3.2 was evaluated. Fig. 10 shows the relationships between the Charpy absorbed energy above the DBTT and the tensile properties (ultimate tensile strength, 0.2% yield stress, total elongation, and reduction in area) at the same test temperature for PW-4, PW-7, and KW-7. The test results at temperatures below the DBTT, where brittle fracture with a very low or zero absorbed energy was detected from the Charpy impact tests, are not included in this figure. As shown in Figs. 10 (a) and (b), the Charpy absorbed energy above the DBTT increased with the ultimate tensile strength and 0.2% yield stress. In contrast, no clear correlations between the absorbed energy and the total elongation and reduction in area were

observed, as shown in Figs. 10 (c) and (d). Therefore, it was possible that a material's strength could directly affect the Charpy absorbed energy above the DBTT. On the other hand, it was not certain whether the total elongation and reduction in area, which were factors that determine a material's ductility, could directly affect the Charpy absorbed energy.

At test temperatures below the DBTT, a higher strength (ultimate tensile strength and 0.2% yield stress) and higher ductility (total elongation and reduction in area) were observed for KW-7 compared to PW-7 from the tensile tests, as mentioned in section 3.2 (see Fig. 4). Moreover, it is known that highly deformed W materials with relatively small grains, such as W foils, narrow rods, and wires, tend to show a higher strength and non-zero elongation (ductility) at low temperatures [29, 30, 50]. Therefore, it was possible that grain refining and K-doping could induce a higher strength and higher ductility in W materials, resulting in a lower DBTT. The details of the effects of grain refining and K-doping on the impact properties are discussed in the next section.

3.3.5 Effect of K-doping

According to several reports on the effects of grain size on the impact properties and fracture toughness of metals, the DBTT could be determined by the grain size (d), and the following Hall–Petch-type relation could be applied [51–53]:

$$\text{DBTT} = A_{\text{DBTT}} - K_{\text{DBTT}} \cdot d^{-1/2} \tag{1}$$

where A_{DBTT} [°C] and K_{DBTT} [°C·µm$^{1/2}$] were constants independent of the grain size. This relation indicated that grain refining could cause a decrease in the DBTT. Although there were very few examples of the application of this relation to W materials, Bonnekoh *et al.* reported that the DBTT of cold-rolled pure W sheets obtained by fracture toughness tests

showed good agreement with this equation [30].

In our previous study [47], not only Eq. (1) but the following equation were shown to fit the experimentally determined DBTT and USE of PW-4, PW-7, and PW-29 very well:

$$\text{USE} = A_{\text{USE}} - K_{\text{USE}} \cdot d^{-1/2} \tag{2}$$

where A_{USE} [J] and K_{USE} [J·μm$^{1/2}$] were constants independent of the grain size. In the present study, to evaluate the effect of grain refining on the Charpy impact properties of pure W and K-doped W fabricated with different production methods and histories and to discuss effects of K-doping on the impact properties of W materials, Eqs. (1) and (2) were applied to KW-7. Fig. 11 shows the relationships between the grain size along the thickness (d_{S}) and the USE and DBTT obtained by Charpy impact tests of KLST specimens (L-S direction) of four materials. The values of d_{S} were 19, 22, 63, and 11 μm for PW-4 [47], PW-7 [47], PW-29 [47], and KW-7 (see Fig. 3). The USEs were the average values of the absorbed energy above the DBTT to 1100 °C. The error bars indicate the difference of the maximum and minimum absorbed energies from the USE. As shown in Fig. 11, Eqs. (1) and (2) also fit the experimentally determined DBTT and USE of KW-7 very well. Thus, in case of W materials fabricated by powder metallurgy, it was possible that the both DBTT and USE from the Charpy impact tests could be predicted by the grain size using Hall–Petch-type relations, even if their production methods and histories were different and if K-doping was or was not used. However, the Hall–Petch-type relations included only the factor of grains. On the other hand, the effect of K-doping was roughly distinguished as the effects of grain refining and dispersion of K-bubbles at the grain boundaries. Therefore, the dispersion of K-bubbles could not directly influence the Charpy impact properties below 1000 °C, although the improvements in the impact properties due to grain refining caused by K-doping were

18

significant. Because the effect of K-doping was originally expected, especially at higher temperatures such as the temperature ranges inducing creep deformation, an investigation of the impact properties at much higher temperatures above 1000 °C is planned as future work to clarify the effect of K-doping in further detail.

3.4 Advantages of K-doped W

As mentioned in section 1, the low temperature brittleness, high DBTT, and recrystallization-induced embrittlement are drawbacks of W materials as the plasma-facing material of a fusion reactor divertor. In the present study, it was clarified that grain refining was a promising method for suppressing the low temperature brittleness and lowering the DBTT. However, it is known that the resistance to recrystallization of most metals becomes lower as the deformation ratio increases [54]. Therefore, the suppression of the low temperature brittleness and high DBTT by an increase in the deformation ratio alone could simultaneously induce recrystallization from a lower temperature range. On the other hand, K-doping could induce grain refining without any increase in the deformation ratio, as mentioned in section 3.1. The grain sizes along all three directions of KW-7 were smaller than those of PW-7 (see Fig. 3). Moreover, according to our previous study [48], the initiation of recrystallization was suppressed in KW-7 (from 1200–1300 °C) compared to PW-7 (from 1100–1200 °C), as shown in Fig. 12. This result indicated the ability to suppress the recrystallization of W materials by K-doping. From the results of these experiments, it was expected that the suppression of the low temperature brittleness, lowering the DBTT, and the suppression of recrystallization of W materials could be simultaneously achieved by K-doping. As a consequence of these advantages, it was possible that a fusion reactor divertor using K-doped W as a plasma-facing material could have a wider operating temperature window than that using conventional pure W.

However, there remain several factors to be considered when determining the availability and applicability of K-doped W as the plasma-facing material of a fusion reactor divertor, which are sputtering, tritium (T) retention, the effects of plasma exposure, high heat flux loading, and neutron irradiation (displacement damage, transmutation, and production of radionuclides), and so on. In our previous simulation study, the lifetime of ITER-like monoblock divertor targets under high heat flux loading up to 20 MW/m^2 by using K-doped W in place of pure W was extended [55]. Because the improvement in the low temperature ductility and the suppression of recrystallization in K-doped W were clarified in the present study, it is possible that the structural strength and lifetime of divertor targets could be improved by using K-doped W. However, these investigations include no consideration of changes in the sputtering coefficient, T retention, and the effects of plasma exposure and neutron irradiation. From the viewpoints of neutron irradiation effects, our previous report showed no difference in irradiation hardening between pure W and K-doped W after neutron irradiation up to about 0.45 dpa at temperatures from 531 °C to 756 °C, which was one of the non-negative effects of K-doping under the neutron irradiation [56]. However, the irradiation dose in that study was very low compared to the expected one (15 dpa per 5 years by Bolt *et al*. [57]). Therefore, high-dose neutron irradiation studies are required in the future. In addition, the production of radionuclides such as ^{39}Ar is a major concern that should be assessed, and the corresponding lifetime should be estimated. Thus, it is important to investigate not only the thermo-mechanical properties reported in this paper but the other important factors described above and to comprehensively evaluate the availability and applicability of K-doped W as the plasma-facing material of a fusion reactor divertor.

4. Conclusion

The grain structure, tensile properties, and Charpy impact properties of pure W and

K-doped W plates fabricated by powder metallurgy and hot rolling were investigated, and the effects of K-doping on the impact properties and the advantages of K-doped W for divertor application in fusion reactors were discussed. The results of this study were summarized as follows:

(1) As positive effects of K-doping, grain refining with no increase in the deformation ratio, an increase in the tensile strength below 1300 °C, an improvement in the ductility (elongation and reduction in area from a tensile test) especially at lower temperatures below the DBTT, and improvements in the Charpy impact properties below 1000 °C were found in the present study.

(2) The K-doped W plate showed an increase in USE of approximately 40% and a decrease in the DBTT of 200 °C compared to pure W with the same deformation ratio.

(3) The improved impact properties of K-doped W were mainly attributed to strengthening by grain refining, which was caused by K-doping during fabrication and not an increase in the deformation ratio. In contrast, effects of the dispersion of K bubbles on the impact properties were not apparent below 1000 °C.

(4) For W materials fabricated by powder metallurgy, the both DBTT and USE from the Charpy impact tests could be predicted by the grain size using Hall–Petch-type relations (DBTT, USE $= A - K \cdot d^{-1/2}$, where A and K were constants independent of the grain size), even if their production methods and histories were different and if K-doping was or was not used.

(5) It was expected that the suppression of the low temperature brittleness, lowering the DBTT, and the suppression of recrystallization, which were issues related to the thermo-mechanical properties of W materials for divertor application in fusion reactors, could be simultaneously improved by K-doping.

Acknowledgements

References

[1] S. Wurster, N. Baluc, M. Battabyal, T. Crosby, J. Du, C. García-Rosales, A. Hasegawa, A. Hoffmann, A. Kimura, H. Kurishita, R. J. Kurtz, H. Li, S. Noh, J. Reiser, J. Riesch, M. Rieth, W. Setyawan, M. Walter, J. -H. You, R. Pippan, J. Nucl. Mater. **442** (2013) S181–S189.

[2] P. Gumbsch, J. Nucl. Mater. **323** (2003) 304–312.

[3] M. Faleschini, H. Kreuzer, D. Kiener, R. Pippan, J. Nucl. Mater. **367–370** (2007) 800–805.

[4] A. Giannattasio, M. Tanaka, T. D. Joseph, S. G. Roberts, Phys. Scr. **T128** (2007) 87–90.

[5] A. Giannattasio, S. G. Roberts, Phil. Mag. **Vol. 87, No. 17** (2007) 2589–2598.

[6] D. Rupp, S. M. Weygand, J. Nucl. Mater. **386–388** (2009) 591–593.

[7] D. Rupp, R. Mönig, P. Gruber, S. M. Weygand, Int. J. Refract. Met. Hard Mater. **28** (2010) 669–673.

[8] D. Rupp, S. M. Weygand, Phil. Mag. **Vol. 90, No. 30**, (2010) 4055–4069.

[9] D. Rupp, S. M. Weygand, J. Nucl. Mater. **417** (2011) 477–480.

[10] E. Gaganidze, D. Rupp, J. Aktaa, J. Nucl. Mater. **446** (2014) 240–245.

[11] A. V. Babak, Strength of Materials **14** (1982) 1389–1391.

[12] N. D. Bega, A. V. Babak, E. I. Uskov Soviet Powder Metallurgy and Metal Ceramics **21** (1982) 408–411.

[13] A. V. Babak, Soviet Powder Metallurgy and Metal Ceramics **22** (1983) 316–318.

[14] A. V. Babak, E. I. Uskov, Strength of Materials **15** (1983) 667–672.

[15] R. C. Rau, J. Moteff, R. L. Ladd, J, Nucl. Mater., 24 (1967) 164–173.

[16] I. V. Gorynin, V. A. Ignatov, V. V. Rybin, S. A. Fabritsiev, V. A. Kazakov, V. P. Chakin, V. A. Tsykanov, V. R. Barabash, Y. G. Prokofyev, J. Nucl. Mater., 191–194 (1992) 421–425.

[17] J. M. Steichen, J. Nucl. Mater., 61 (1976) 13–19.

[18] P. Krautwasser, H. Derz, E. Kny, Proc. 12th International PLANSEE Seminar (1989) 673–681.

[19] K. Farrell, A. C. Schaffhauser, J. O. Stiegler, J. Less-Common Met. **13** (1967) 141–155.

[20] Q. Wei and L. J. Kecskes, Mater. Sci. Eng. A **491** (2008) 62–69.

[21] A. Luo, K. S. Shin, D. L. Jacobson, Scr. Metall. **25** (1991) 2411–2414.

[22] P. Makarov and K. Povarova, Int. J. Refract. Met. Hard Mater. **20** (2002) 277–285.

[23] P. Schade, Int. J. Refract. Met. H 28 (2010) 648–660.

[24] J. W. Pugh, Metall. Trans. A **4** (1973) 533–538.

[25] P. K. Wright, Metall. Trans. A **9** (1978) 955–963.

[26] D. B. Snow, Metall. Trans. A **10** (1979) 815–821.

[27] E. O. Hall, Proc. Phys. Soc. London Sect. B **64** (1951) 747–753.

[28] N. J. Petch, J. Iron Steel Inst., London **173** (1953) 25–28.

[29] K. Farrell, A. C. Schaffhauser, J. O. Stiegler, J. Less-Common Met. **13** (1967) 141–155.

[30] C. Bonnekoh, A. Hoffmann, J. Reiser, Int. J. Refract. Met. Hard Mater. **71** (2018) 181–189.

[31] G. Pintsuk, I. Uytdenhouwen, Int. J. Refract. Met. Hard Mater. 28 (2010) 661–668.

[32] H. Sheng, I. Uytdenhouwen, G. Van Oost, J. Vleugels, Nucl. Eng. Des. 246 (2012) 198–202.

[33] M. Fukuda, S. Nogami, K. Yabuuchi, A. Hasegawa, T. Muroga, Fus. Sci. Tech. **68** (2015) 690–693.

[34] W. H. Guan, S. Nogami, M. Fukuda, A. Hasegawa, Fus. Eng. Des. **109–111** (2016) 1538–1542.

[35] S. Nogami, W. H. Guan, M. Fukuda, A. Hasegawa, Fus. Eng. Des. **109–111** (2016) 1549–1553.

[36] S. Nogami, W. H. Guan, A. Hasegawa, M. Fukuda, Fus. Sci. Tech. **72** (2017) 673–679.

[37] K. Sasaki, K. Yabuuchi, S. Nogami, A. Hasegawa, J. Nucl. Mater. **461** (2015) 357–364.

[38] A. Hasegawa, M. Fukuda, T. Tanno, S. Nogami, K. Yabuuchi, T. Tanaka, T. Muroga, Proc. of 25th IAEA Fusion Energy Conference, MPT02, (2014).

[39] M. Rieth, A. Hoffmann, Int. J. Refract. Met. Hard Mater. **28** (2010) 679–686.

[40] M. Rieth, A. Hoffmann, Advances in Science and Technology **59** (2008) 101–104.

[41] ASTM E112–85, Standard Methods for Determining the Average Grain Size, Annual Book of ASTM, 1986, 227–290.

[42] DIN EN ISO 14556:2017-05, Metallische Werkstoffe - Kerbschlagbiegeversuch nach Charpy (V-Kerb) - Instrumentiertes Prüfverfahren (ISO 14556:2015); Deutsche Fassung EN ISO 14556:2015 [in German].

[43] J. Reiser, M. Rieth, B. Dafferner, A. Hoffmann, J. Nucl. Mater. **442** (2013) S204–S207.

[44] J. Reiser, L. Garrison, H. Greuner, J. Hoffmann, T. Weingärtner, Ute Jäntsch, M. Klimenkov, P. Franke, S. Bonk, C. Bonnekoh, S. Sickinger, S. Baumgärtner, D. Bolich, M. Hoffmann, R. Ziegler, J. Konrad, J. Hohe, A. Hoffmann, T. Mrotzek, M. Seiss, M. Rieth, A. Möslang, Int. J. Refract. Met. Hard Mater. **69** (2017) 66–109.

[45] M. Rieth, D. Armstrong, B. Dafferner, S. Heger, A. Hoffmann, M.-D. Hoffmann, U. Jäntsch, C. Kübel, E. Materna-Morris, J. Reiser, M. Rohde, T. Scherer, V. Widak, H. Zimmermann, Advances in Science and Technology **73** (2010) 11–21.

[46] M. Rieth, J, Reiser, B. Dafferner, S, Baumgärtner, Fus. Sci. Technol. **61** (2012) 381–384.

[47] S. Nogami, S. Watanabe, J. Reiser, M. Rieth, S. Sickinger, A. Hasegawa, Fus. Eng. Des. **135** (2018) 196–203.

[48] K. Tsuchida, T. Miyazawa, A. Hasegawa, S. Nogami, M. Fukuda, Nucl. Mater. Energy **15** (2018) 158–163.

[49] D. A. Curry and J. F. Knott, Met. Sci. 12 (1978) 511–514.

[50] D. Lee, Metall. Trans. A 6 (1975) 2083–2088.

[51] N. J. Petch, Philos. Mag. **3** (1958) 1089.

[52] A. N. Stroh, Adv. Phys. **6** (1957) 48.

[53] T. Hanamura, F. Yin, K. Nagai, ISIJ Int. **44** (2004) 610–617.

[54] H. Takahashi, H. Uetsuka, T. Takeyama, The Effect of the Recovery and Recrystallization Processes on the Mechanical Properties of a Mild Steel, Bulletin of the Faculty of Engineering, Hokkaido University, **75** (1975) 193–202 [in Japanese].

[55] S. Nogami, W. H. Guan, T. Hattori, K. James, A. Hasegawa, Phys. Scr. **T170** (2017) 014011.

[56] M. Fukuda, A. Hasegawa, S. Nogami, K. Yabuuchi, J. Nucl. Mater. **449** (2014) 213–218.

[57] H. Bolt, V. Barabash, G. Federici, J. Linke, A. Loarte, J. Roth, K. Sato, J. Nucl. Mater. **307–311** (2002) 43–52.

Table 1 Ultimate tensile strength (UTS), 0.2% yield stress ($\sigma_{0.2}$), total elongation (T.E.), reduction in area (R.A.), and fracture manner by tensile tests along S direction of as-received pure W plate (7 mm thick) and as-received K-doped W plate (7 mm thick) under strain rates of 1×10^{-3} s^{-1} and 1×10^{-1} s^{-1} and test temperatures of R.T. and 700 °C.

Material	Direction	Strain rate [s^{-1}]	Test temp. [°C]	UTS [MPa]	$\sigma_{0.2}$ [MPa]	T.E. [%]	R.A. [%]	Fracture manner
Pure W (7 mm thick)	S	10^{-3}	R.T.	193	–	0	0	CV
			700	534	490	5	0	IG-SGB
		10^{-1}	R.T.	135	–	0	0	IG-SGB
			700	276	–	0	0	IG-SGB
K-doped W (7 mm thick)	S	10^{-3}	R.T.	235	–	0	0	IG-SGB
			700	579	548	28	0	IG-SGB
		10^{-1}	R.T.	138	–	0	0	IG-SGB
			700	390	–	0	0	IG-SGB

CV: cleavage, SGB: intergranular fracture at sub-grain boundary

Fig. 1 Shape and dimensions of (a) SS-J tensile specimen, (b) VS-T tensile specimen, and (c) KLST Charpy V-notched specimen and (d) nomenclature of directions of materials and specimens.

(a) SS-J tensile specimen

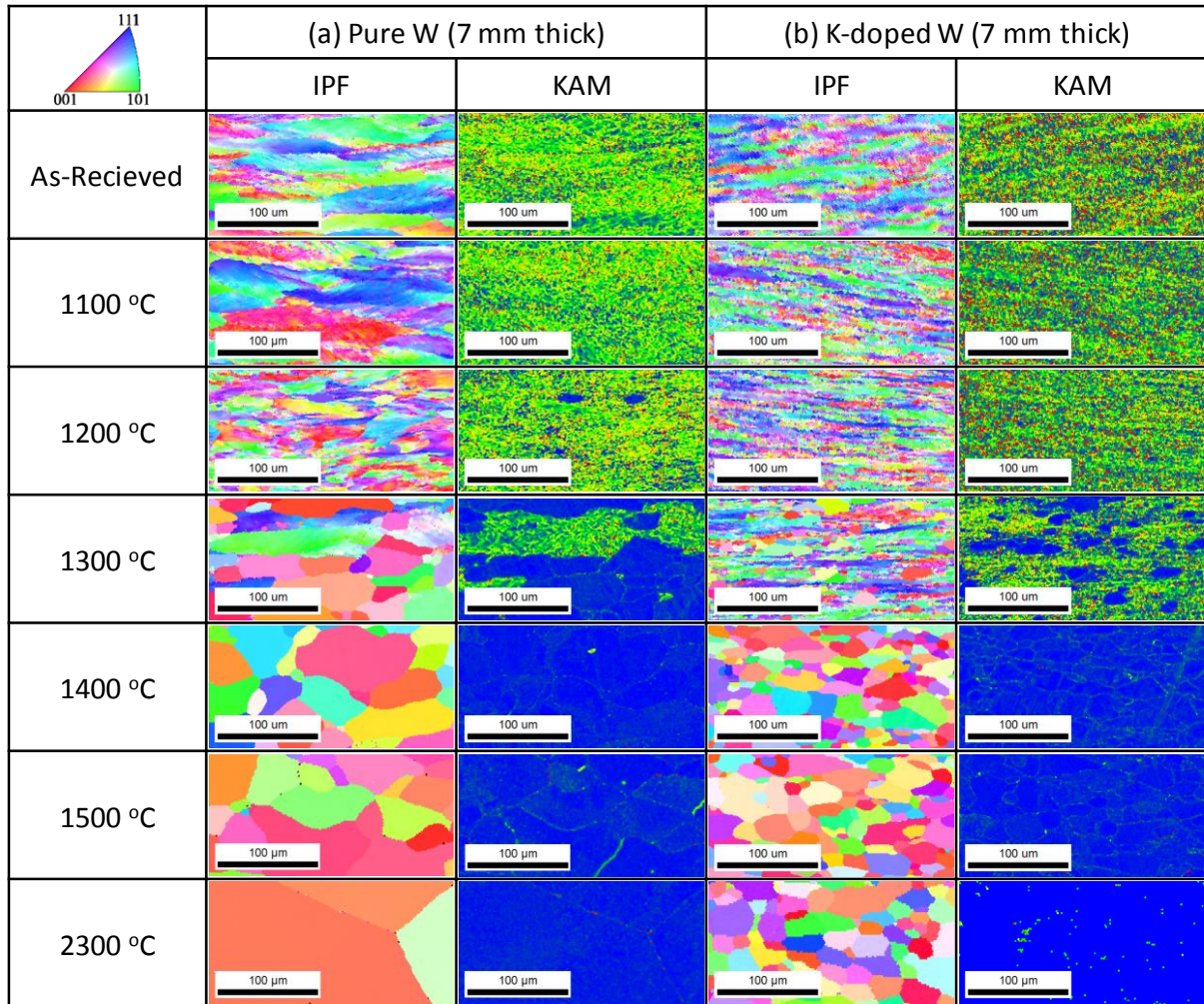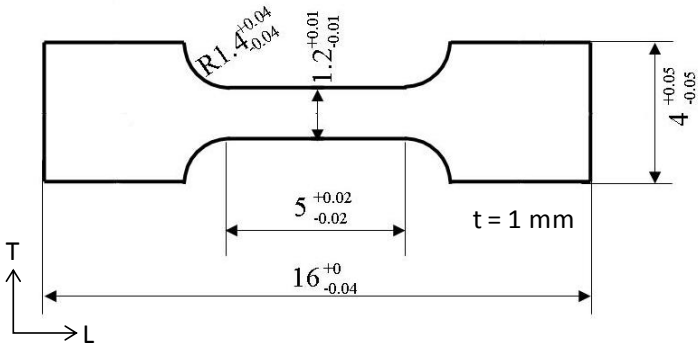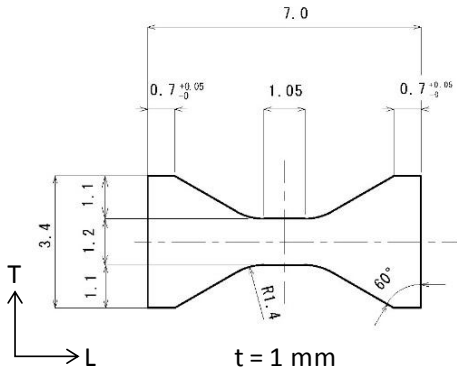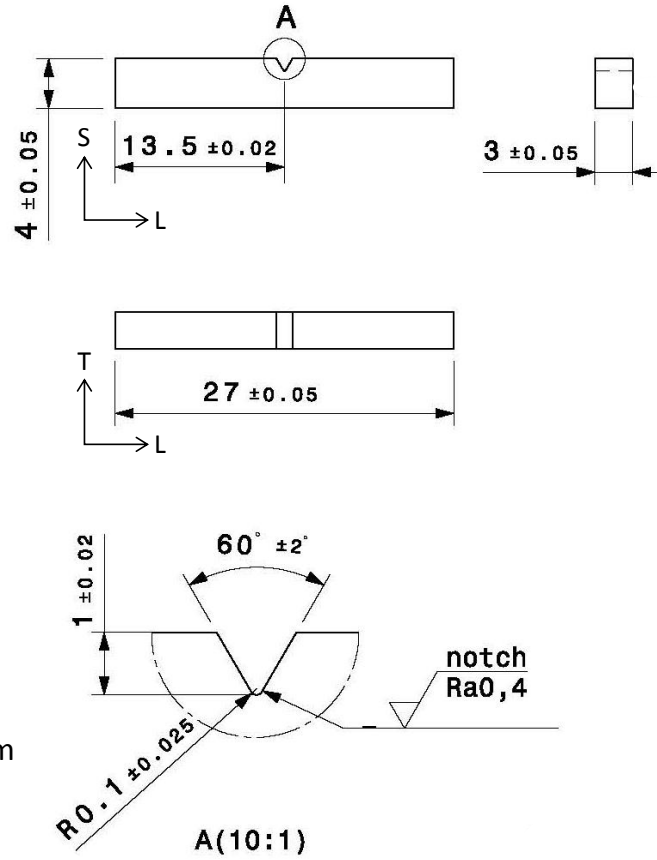(b) VS-T tensile specimen

(c) KLST Charpy impact specimen

Unit: mm

(d)
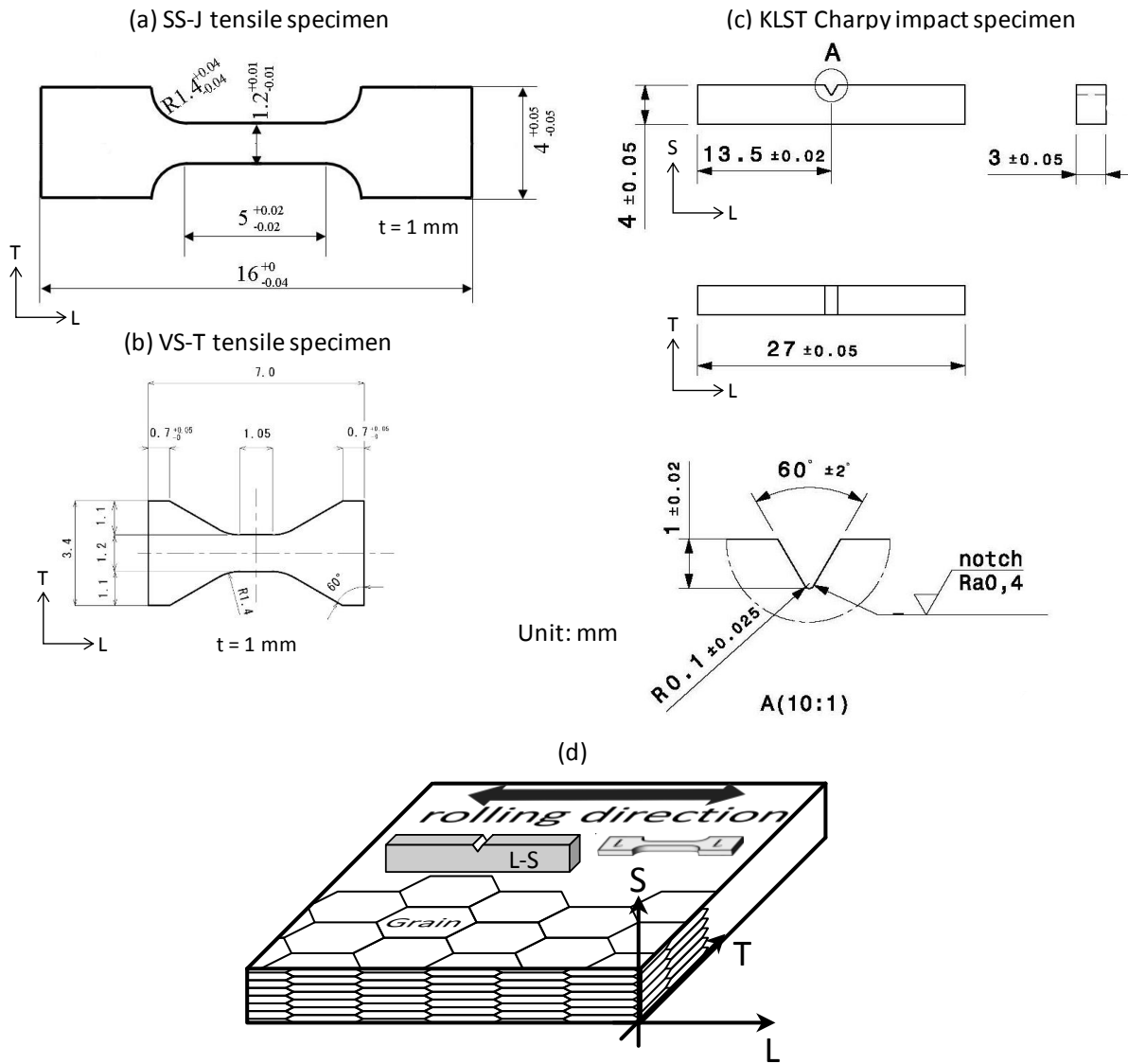
Fig. 2 3D metallographic images and 3D inverse pole figure (IPF) images obtained by electron backscatter diffraction (EBSD) analyses after electrolytic polishing of (a) as-receive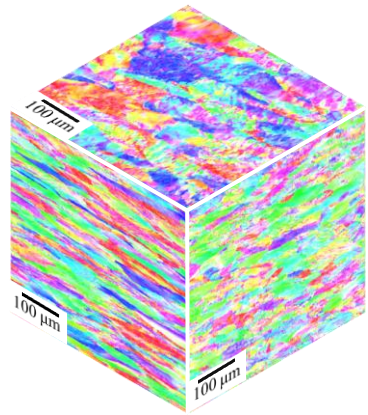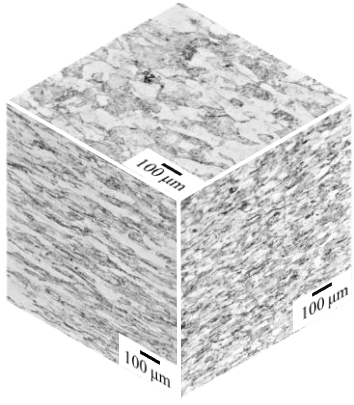d pure W plate (4 mm thick), (b) as-received pure W plate (7 mm thick) [47], and (c) as-received K-doped W plate (7 mm thick).
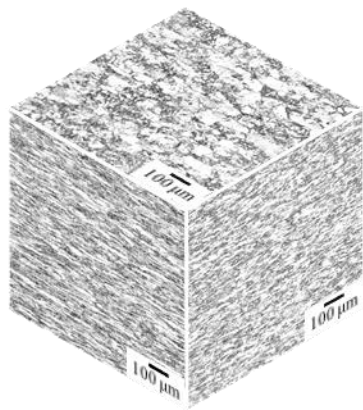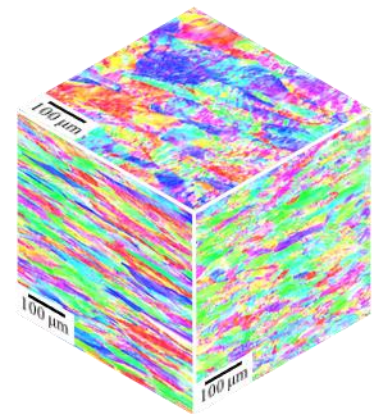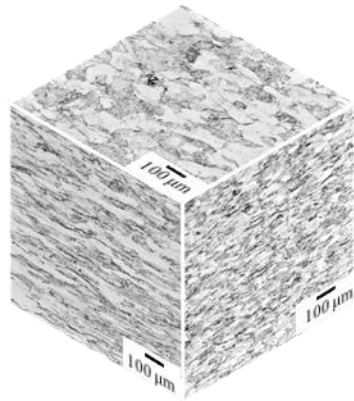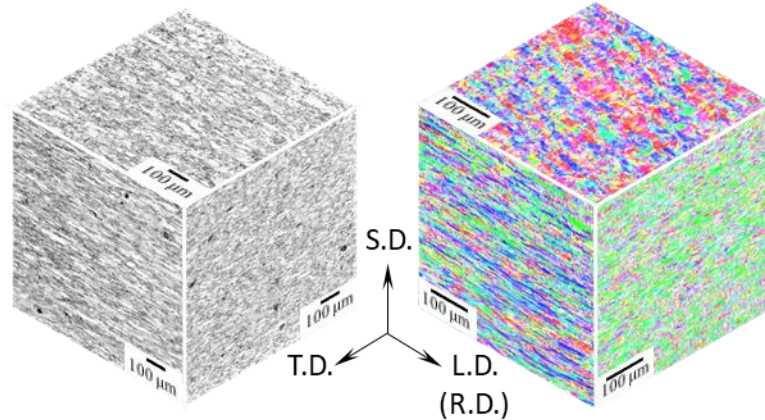
Fig. 3 Average grain sizes along L, T, and S directions (d_L, d_T, and d_S) of as-received pure W plate (4 mm thick) [47], as-received pure W plate (7 mm thick) [47], and as-received K-doped W plate (7 mm thick).
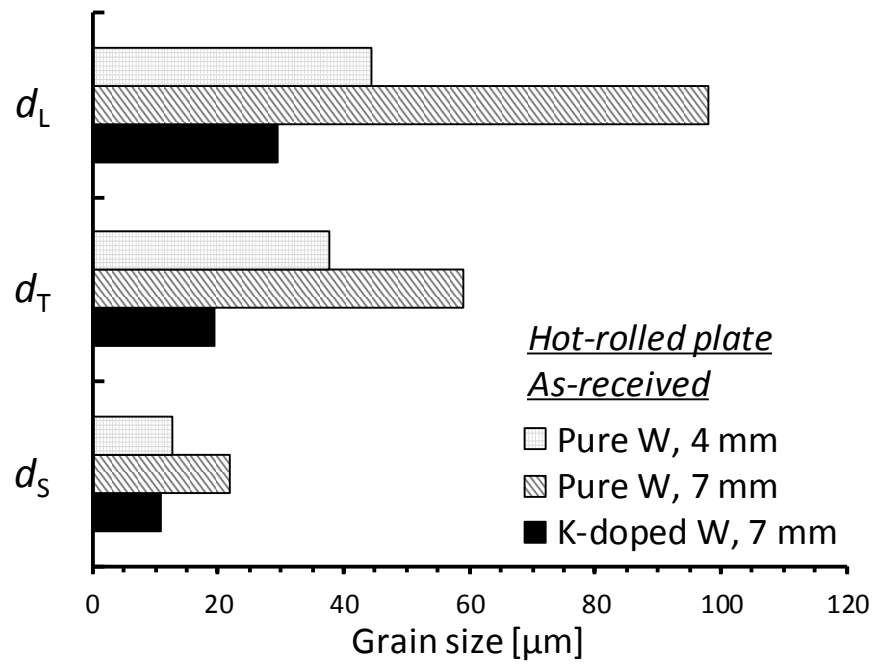
Fig. 4 Test temperature dependences of (a) ultimate tensile strength, (b) 0.2% yield stress, (c) total elongation, and (d) reduction in area by tensile tests (strain rate = 1×10^{-3} s^{-1}) using SS-J specimens along L direction of as-received pure W plate (4 mm thick), as-received pure W plate (7 mm thick) [33, 37, 38], and as-received K-doped W plate (7 mm thick) [33, 37, 38].
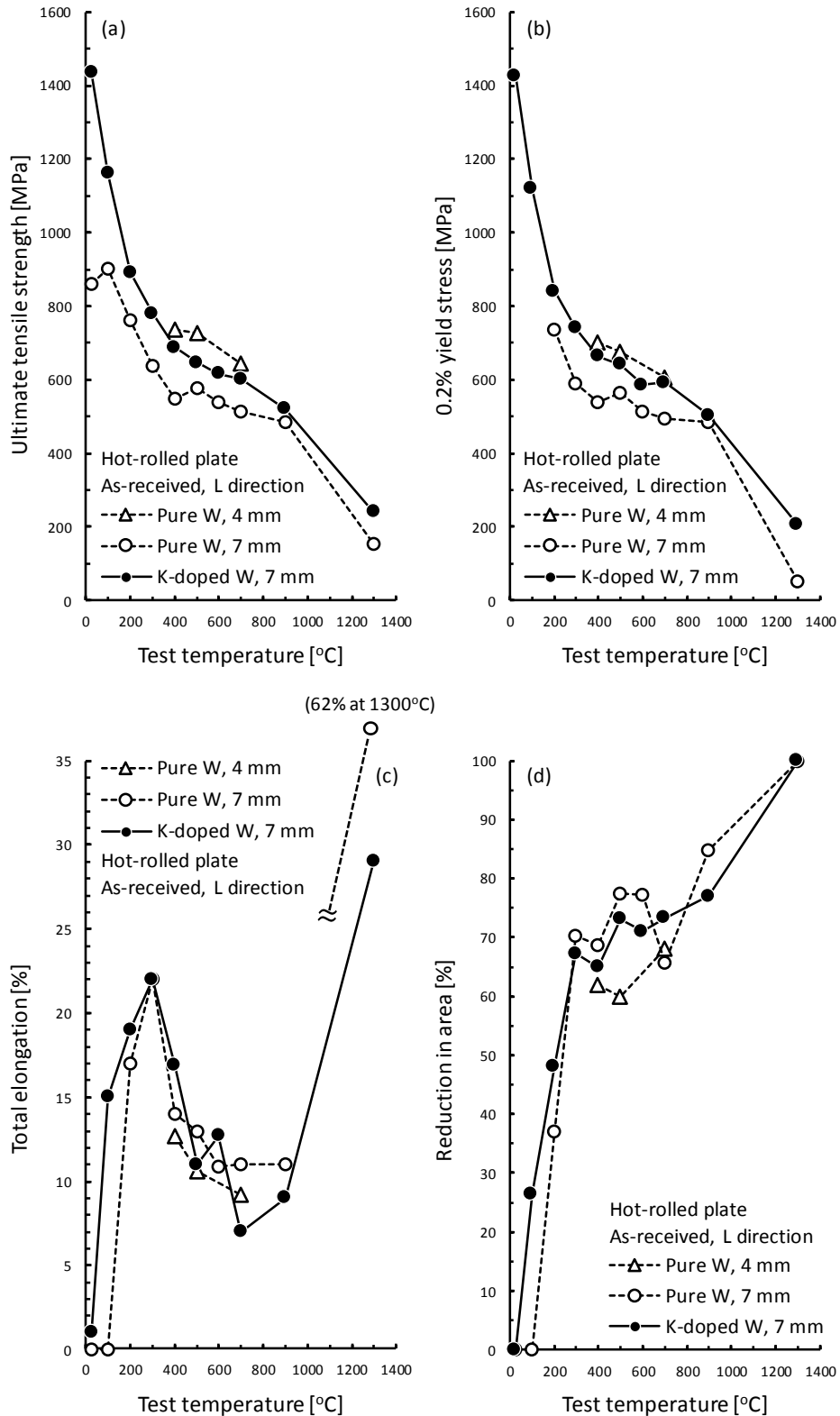
Fig. 5 Test temperature dependences of absorbed energy from Charpy impact tests of KLST specimens (L-S direction) of as-received pure W plate (4 mm thick) [39, 40, 43–45], as-received pure W plate (7 mm thick) [47], as-received pure W round-blank (175 mm diameter and 29 mm thickness) [45, 46], and as-received K-doped W plate (7 mm thick).
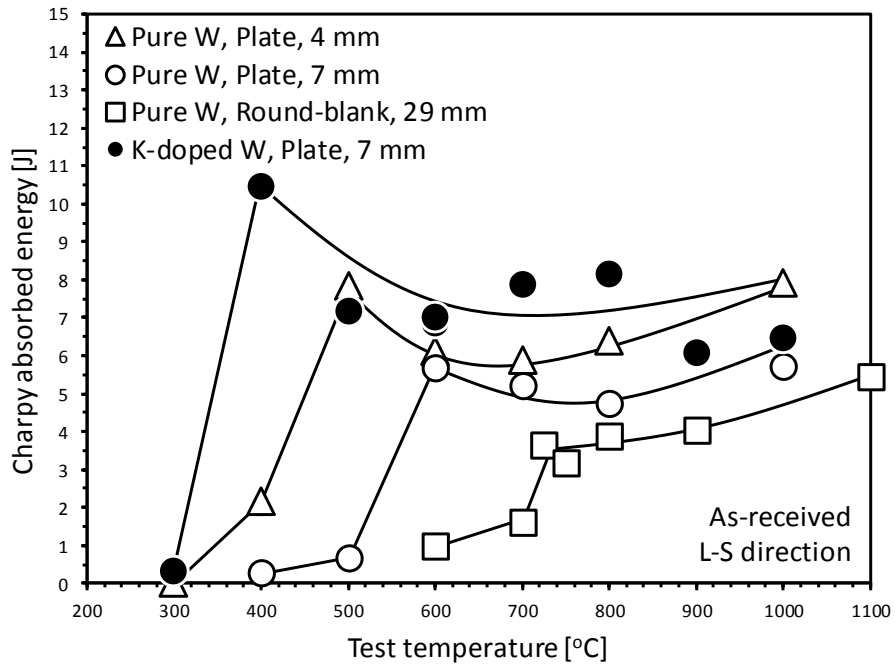
Fig. 6 Relationship between USE and DBTT obtained by Charpy impact tests of KLST specimens (L-S direction) of as-received pure W plate (4 mm thick) [39, 40, 43–45], as-received pure W plate (7 mm thick) [47], as-received pure W round-blank (175 mm diameter and 29 mm thickness) [45, 46], and as-received K-doped W plate (7 mm thick). The USEs are the average values of absorbed energy above DBTT and below 1100 °C.
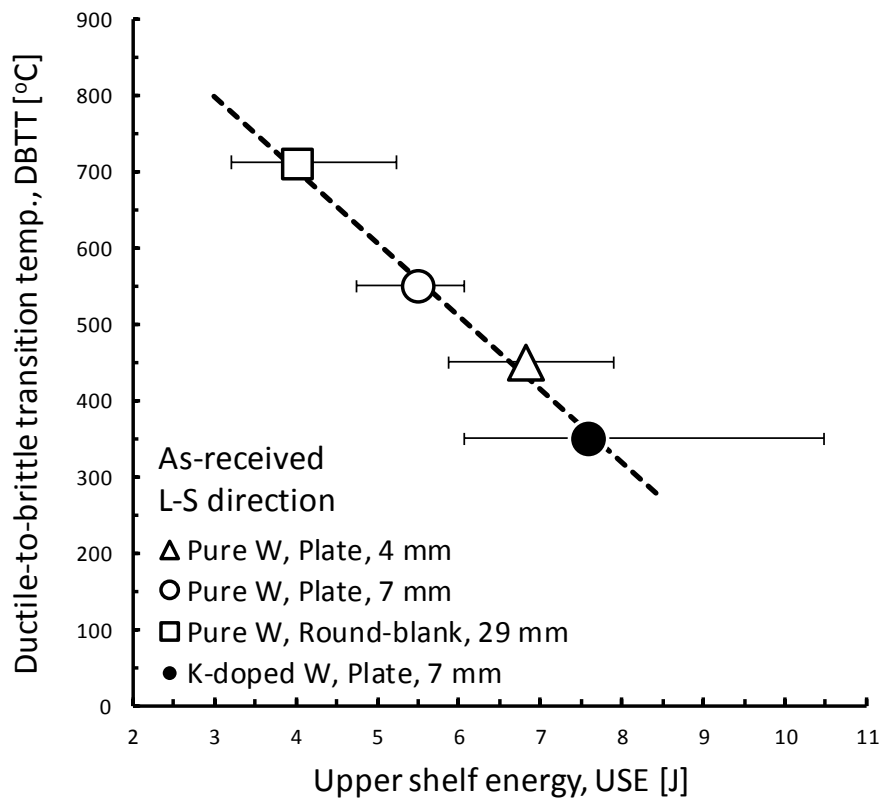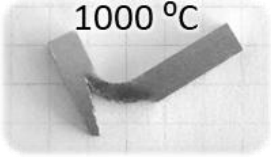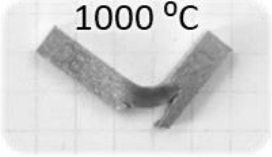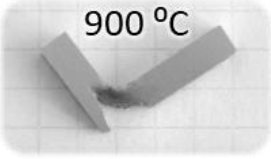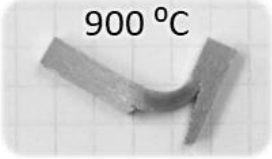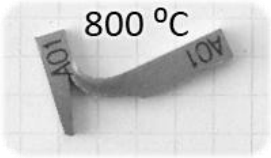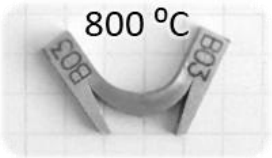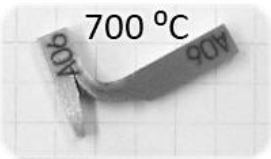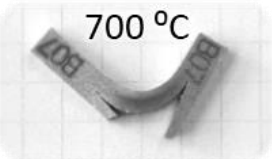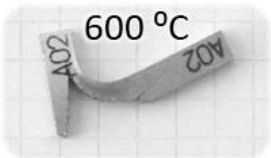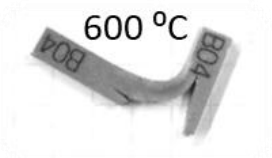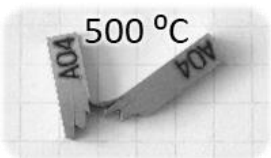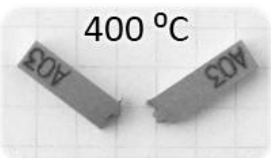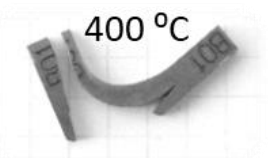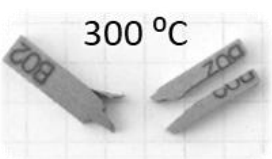
Fig. 7 Appearances of KLST specimens after Charpy impact tests (L-S direction) of (a) as-received pure W plate (7 mm thick) [47] and (b) as-received K-doped W plate (7 mm thick). Descriptions in the right column for each specimen indicate fracture manner.

(a) Pure W (7 mm)		(b) K-doped W (7 mm)	
1000 °C	Del.	1000 °C	Del.
900 °C	Del.	900 °C	Del.
800 °C	Del.	800 °C	Del.
700 °C	Del.	700 °C	Del.
600 °C	Del.	600 °C	Del.
500 °C	Del. + Bri.	500 °C	Del.
400 °C	Bri.	400 °C	Del.
		300 °C	Del. + Bri.

* Del.: Delamination, Bri.: Brittle fracture

Fig. 8 Fracture surfaces of specimens after Charpy impact tests (L-S direction) of as-received pure W plate (7 mm thick) tested at (a) 900 °C and (b) 400 °C and as-received K-doped W plate (7 mm thick) tested at (c) 800 °C and (d) 300 °C.

(a) Pure W (7 mm) / 900 °C

(c) K-doped W (7 mm) / 800 °C

(b) Pure W (7 mm) / 400 °C

(d) K-doped W (7 mm) / 300 °C
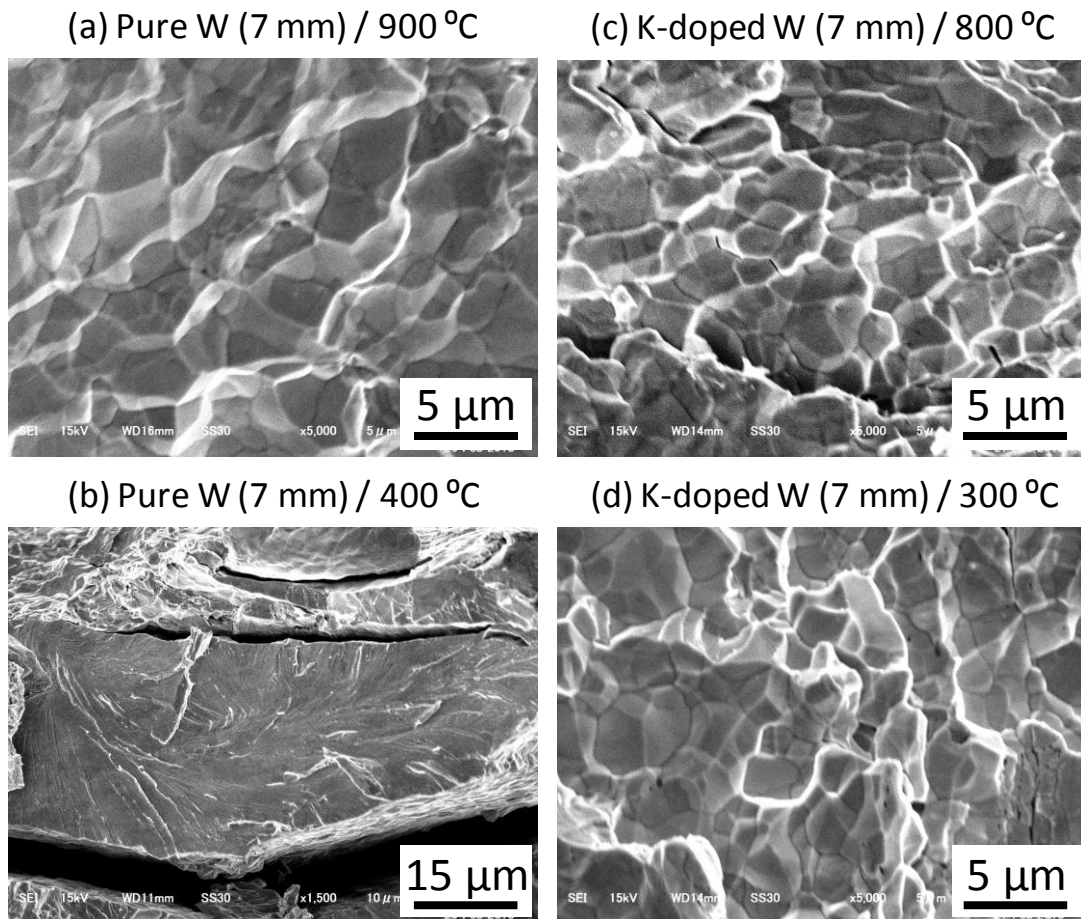
Fig. 9 Fracture surfaces of specimens after tensile tests along S direction of as-received pure W plate (7 mm thick) and as-received K-doped W plate (7 mm thick). Test temperature and strain rate are (a, e) R.T. and 1×10^{-3} s^{-1}, (b, f) 700 °C and 1×10^{-3} s^{-1}, (c, g) R.T. and 1×10^{-1} s^{-1}, (d, h) 700 °C and 1×10^{-1} s^{-1}, respectively.

(a) Pure W (7 mm) / R.T. / 10^{-3} s^{-1}
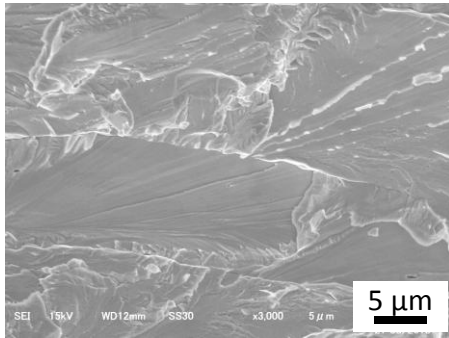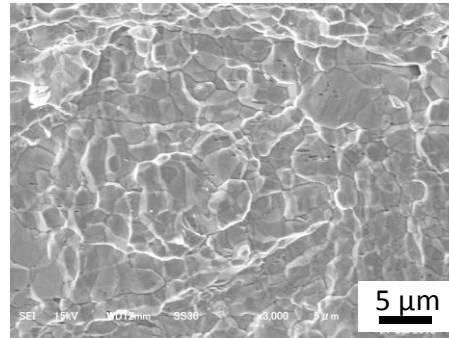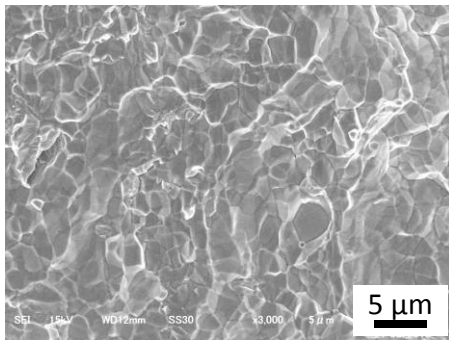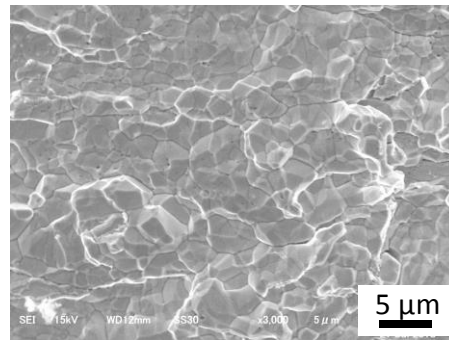
(e) K-doped W (7 mm) / R.T. / 10^{-3} s^{-1}

(b) Pure W (7 mm) / 700 °C / 10^{-3} s^{-1}

(f) K-doped W (7 mm) / 700 °C / 10^{-3} s^{-1}
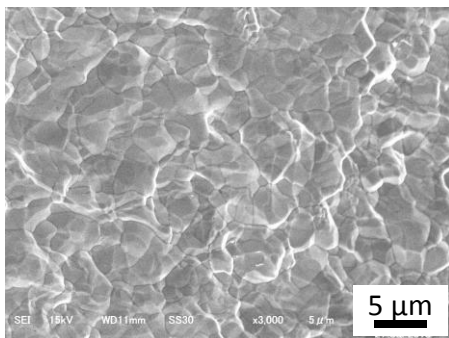
(c) Pure W (7 mm) / R.T. / 10^{-1} s^{-1}

(g) K-doped W (7 mm) / R.T. / 10^{-1} s^{-1}
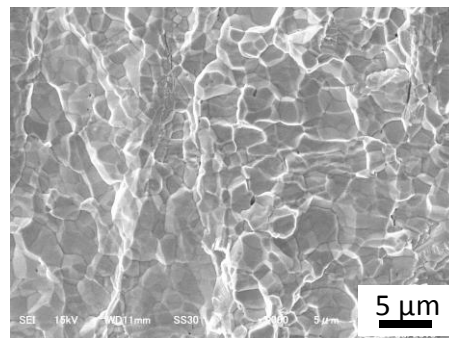
(d) Pure W (7 mm) / 700 °C / 10^{-1} s^{-1}
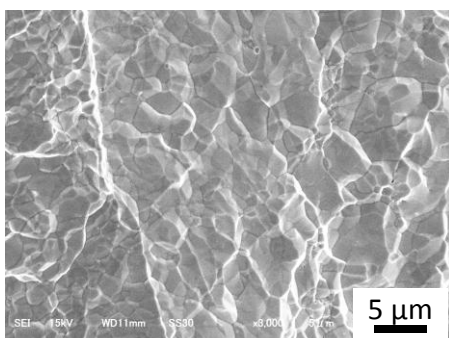
(h) K-doped W (7 mm) / 700 °C / 10^{-1} s^{-1}
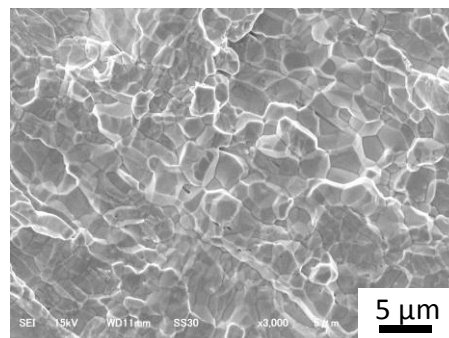
Fig. 10 Relationships between Charpy absorbed energy above DBTT and tensile properties ((a) ultimate tensile strength, (b) 0.2% yield stress, (c) total elongation, and (d) reduction in area) at the same test temperature for as-received pure W plate (4 mm thick) [39, 40, 43–45, 47], as-received pure W plate (7 mm thick) [33, 37, 38, 47], and as-received K-doped W plate (7 mm thick) [33, 37, 38]. Charpy absorbed energy is obtained by Charpy impact tests of KLST specimens (L-S direction). Tensile test is performed using SS-J specimens along L direction under strain rate of 1×10^{-3} s^{-1}.
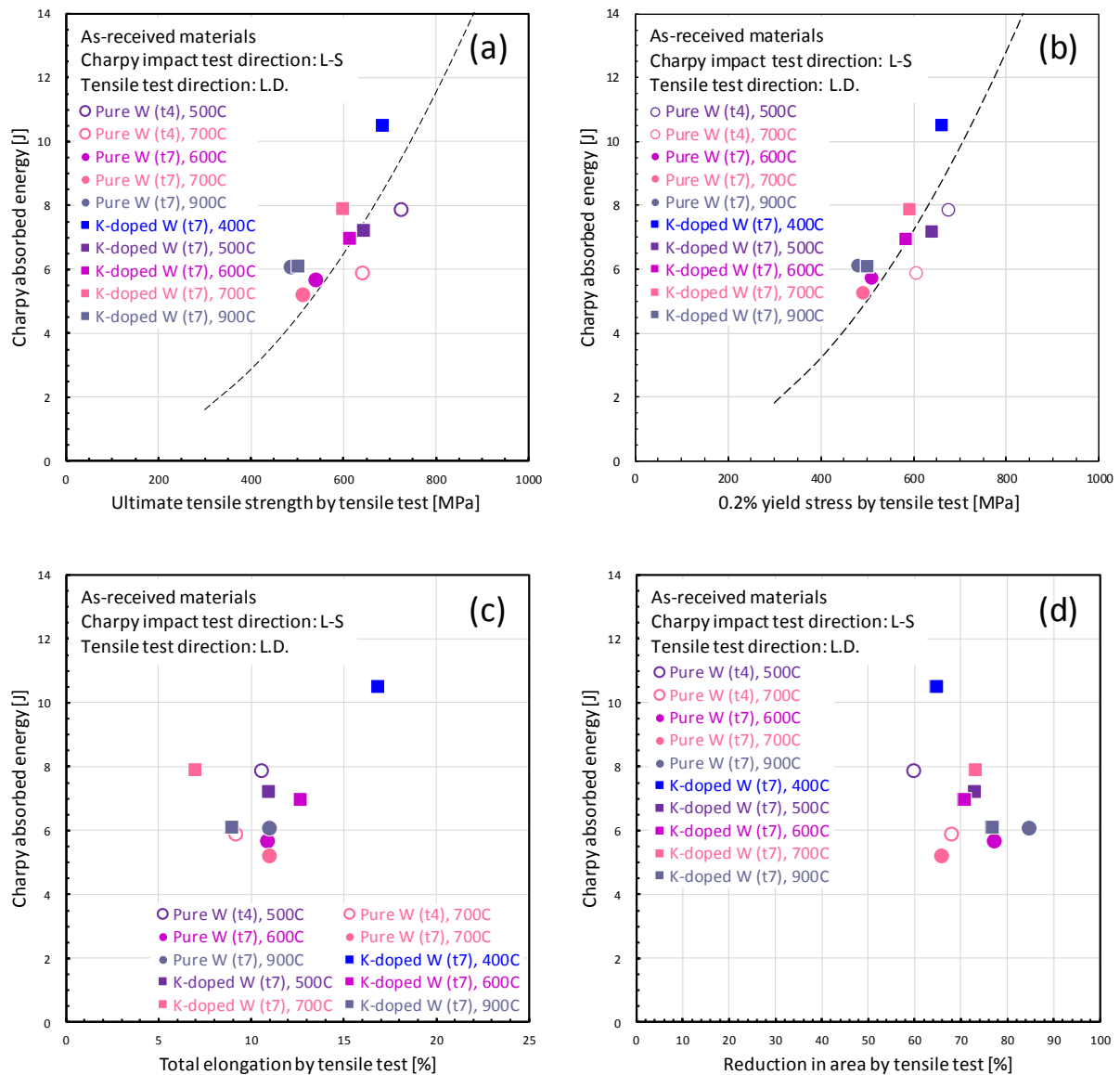
Fig. 11 Relationships between grain size along thickness (d_S) and USE and DBTT obtained by Charpy impact tests of KLST specimens (L-S direction) of as-received pure W plate (4 mm thick) [39, 40, 43–45, 47], as-received pure W plate (7 mm thick) [47], as-received pure W round-blank (175 mm diameter and 29 mm thickness) [45–47], and as-received K-doped W plate (7 mm thick). The USEs are the average values of absorbed energy above DBTT and below 1100 °C.
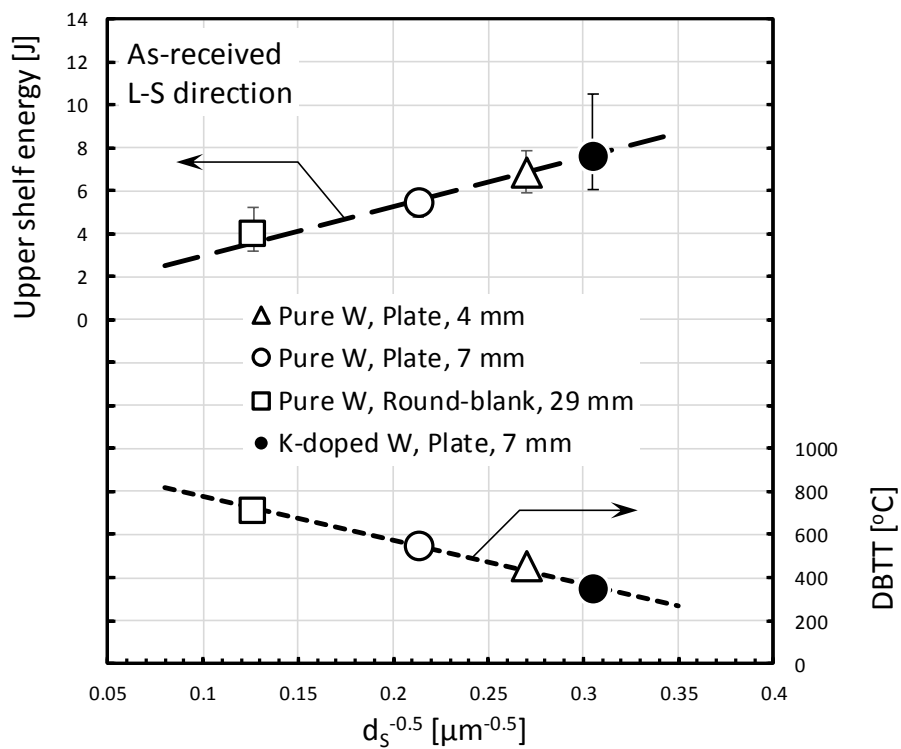
Fig. 12 Inverse pole figures (IPF) and Kernel average misorientation (KAM) images obtained by electron backscatter diffraction (EBSD) analyses of (a) pure W plate (7 mm thick) and (b) K-doped W plate (7 mm thick) in as-received condition and after heat treatment at 1100 °C, 1200 °C, 1300 °C, 1400 °C, 1500 °C, and 2300 °C for 1 h in vacuum [48].

(a) SS-J tensile specimen

$R1.4^{+0.04}_{-0.04}$ $1.2^{+0.01}_{-0.01}$ $4^{+0.05}_{-0.05}$

$5^{+0.02}_{-0.02}$ t = 1 mm

$16^{+0}_{-0.04}$

T

L

(b) VS-T tensile specimen

7. 0

$0.7^{+0.05}_{-0}$ 1. 05 $0.7^{+0.05}_{-0}$

3. 4 1. 1 1. 2 1. 1 1. 1

R1.4 60°

T

L t = 1 mm

(c) KLST Charpy impact specimen

A

4 ± 0.05 S 13.5 ± 0.02 L 3 ± 0.05

T 27 ± 0.05 L

1 ± 0.02 $60° \pm 2°$

notch
Ra0,4

R0.1 ±0.025

Unit: mm

A(10:1)

(d)

rolling direction

L-S

Grain

S

T

L
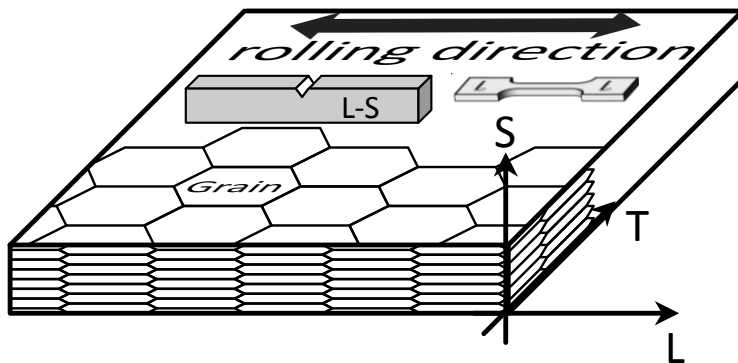
Fig. 2
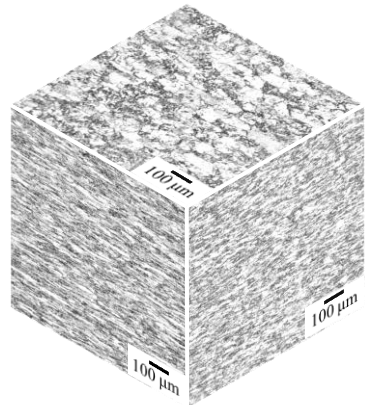
(a) Pure W plate (4 mm thick) (b) Pure W plate (7 mm thick)

(c) K-doped W plate (7 mm thick)

S.D.

T.D. L.D.
(R.D.)

Fig. 3

Fig. 4

Fig. 5

Fig. 6
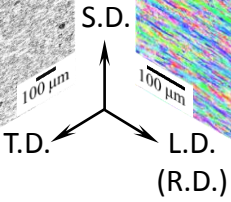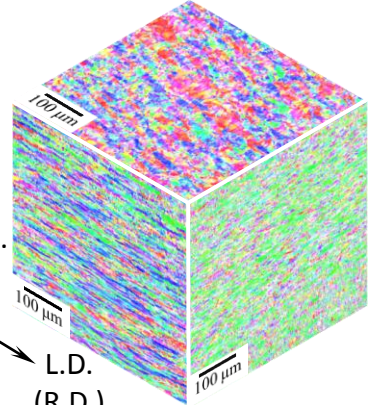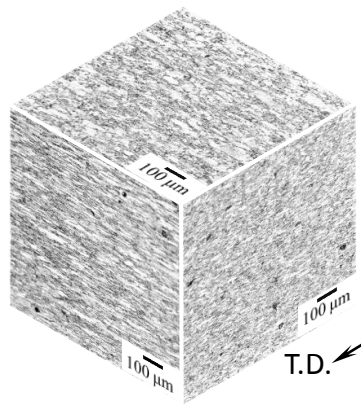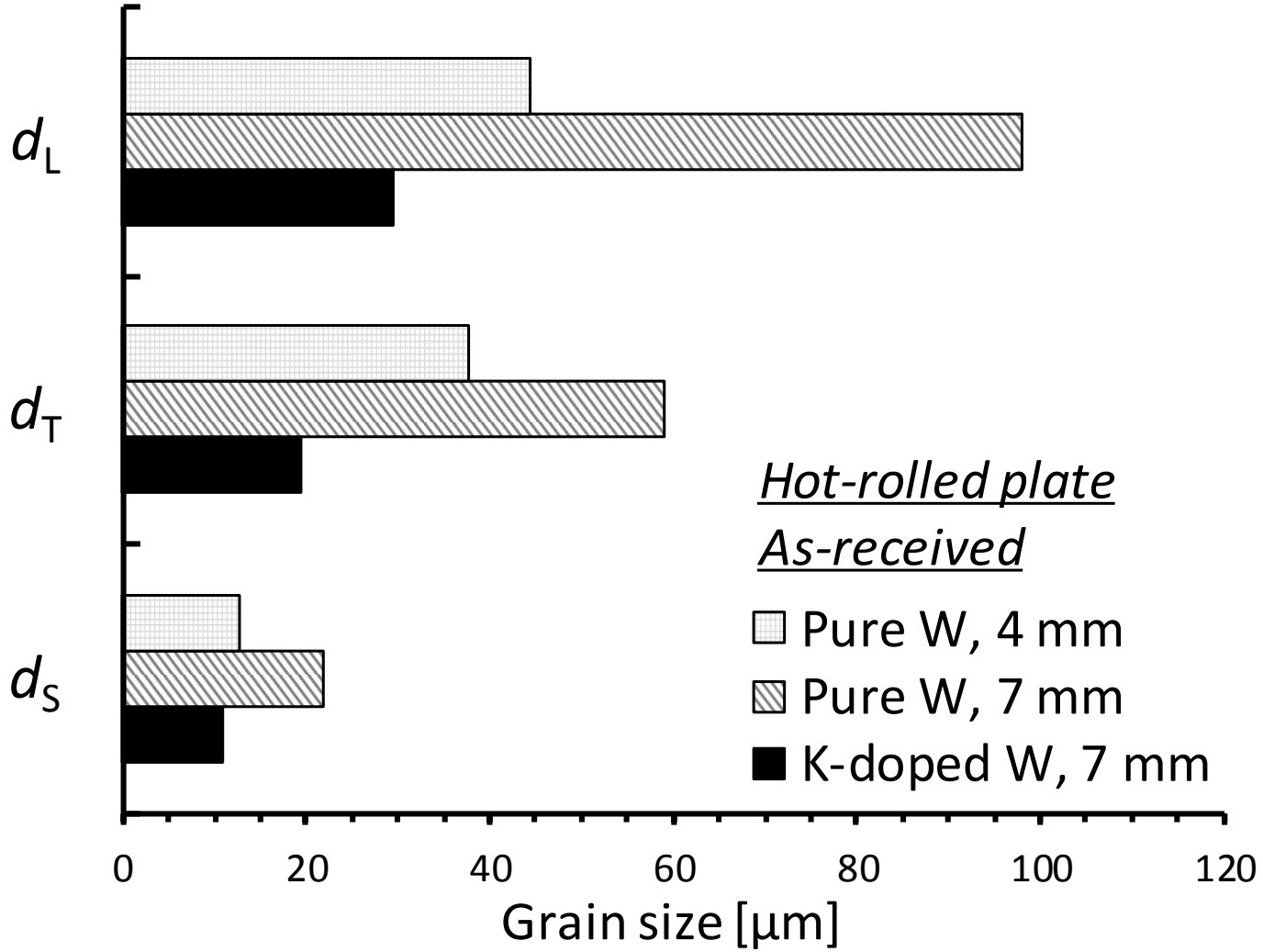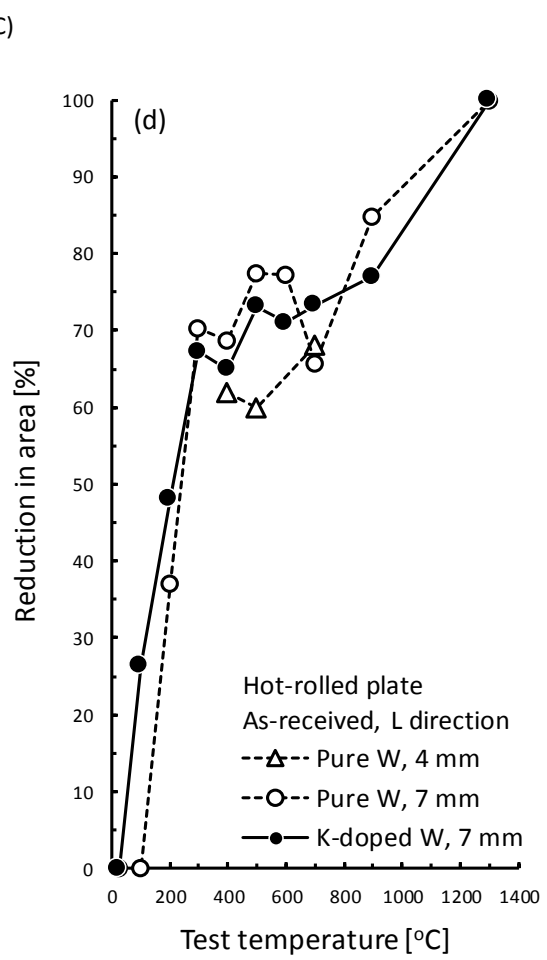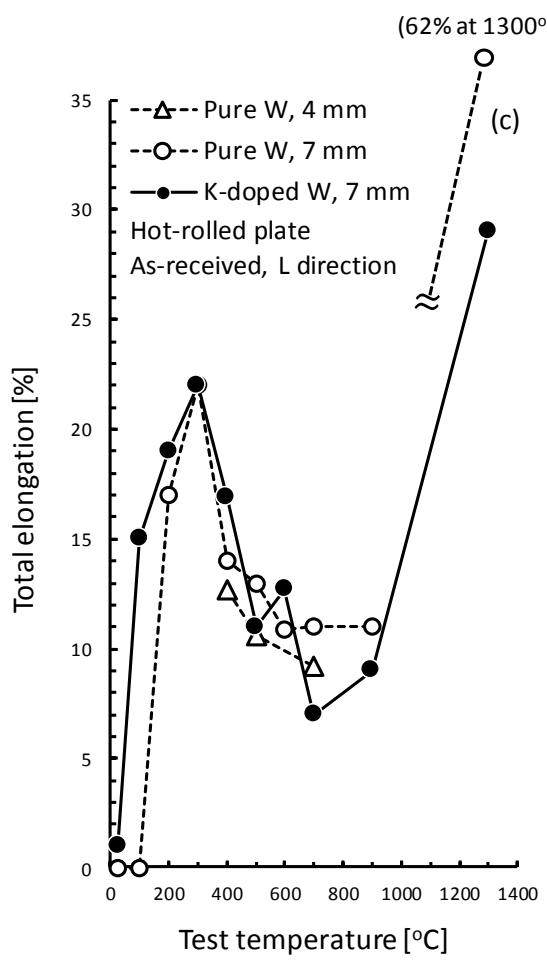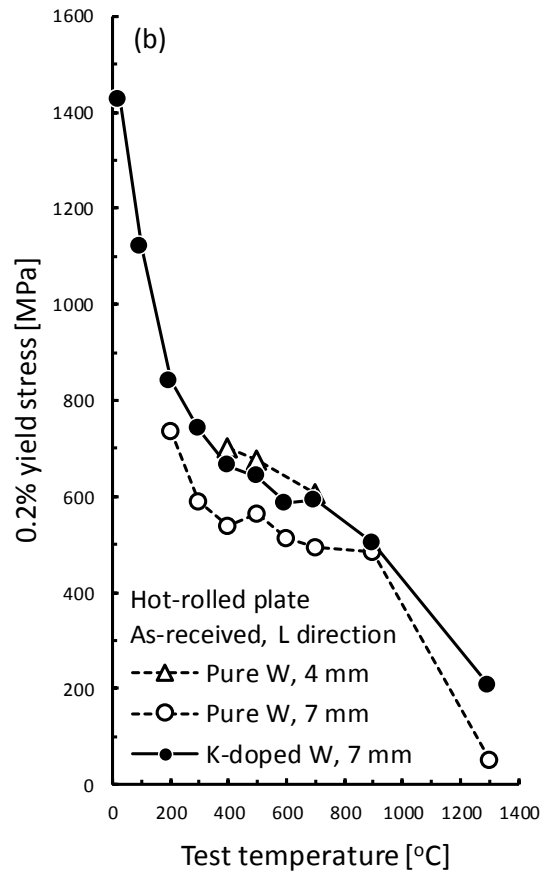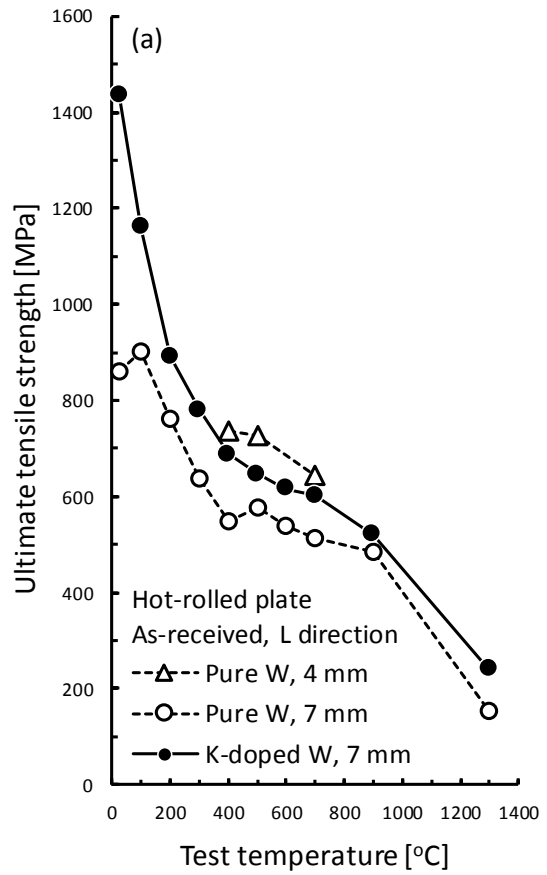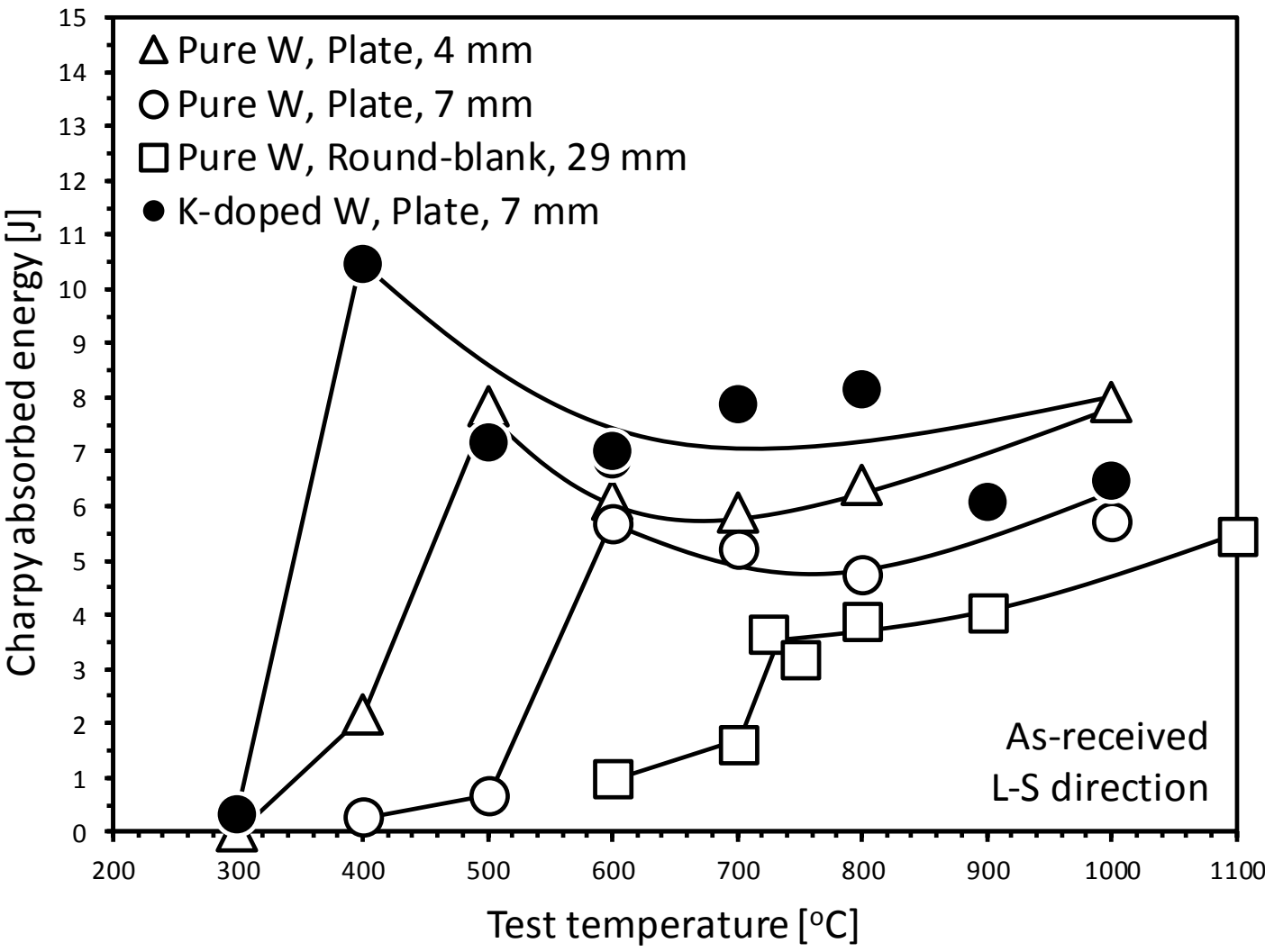
Fig. 6. Ductile-to-brittle transition temperature, DBTT [°C], versus Upper shelf energy, USE [J], for as-received L-S direction samples:
- △ Pure W, Plate, 4 mm
- ○ Pure W, Plate, 7 mm
- □ Pure W, Round-blank, 29 mm
- ● K-doped W, Plate, 7 mm
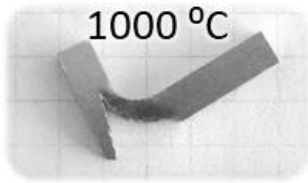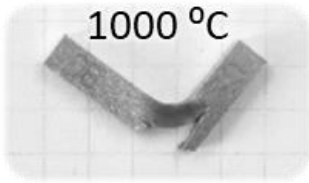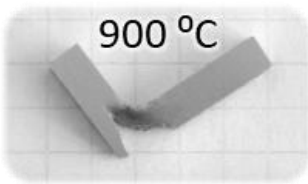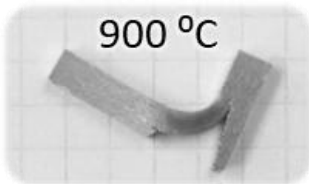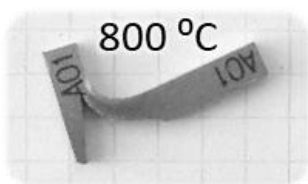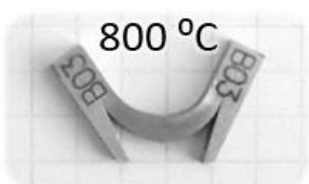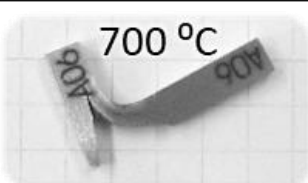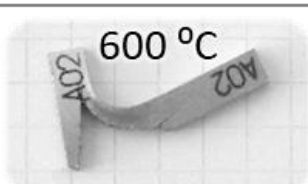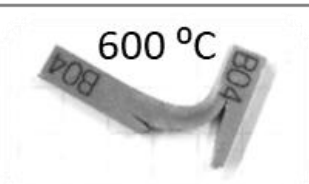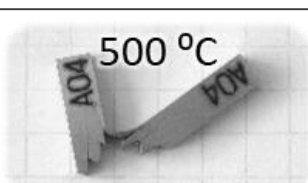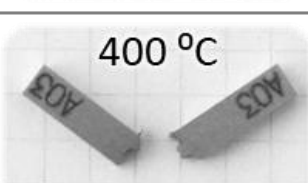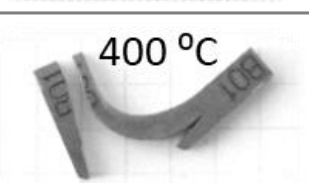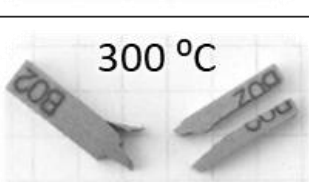
Fig. 7

(a) Pure W (7 mm)		(b) K-doped W (7 mm)	
1000 °C	Del.	1000 °C	Del.
900 °C	Del.	900 °C	Del.
800 °C	Del.	800 °C	Del.
700 °C	Del.	700 °C	Del.
600 °C	Del.	600 °C	Del.
500 °C	Del. + Bri.	500 °C	Del.
400 °C	Bri.	400 °C	Del.
		300 °C	Del. + Bri.

* Del.: Delamination, Bri.: Brittle fracture

Fig. 8

(a) Pure W (7 mm) / 900 °C
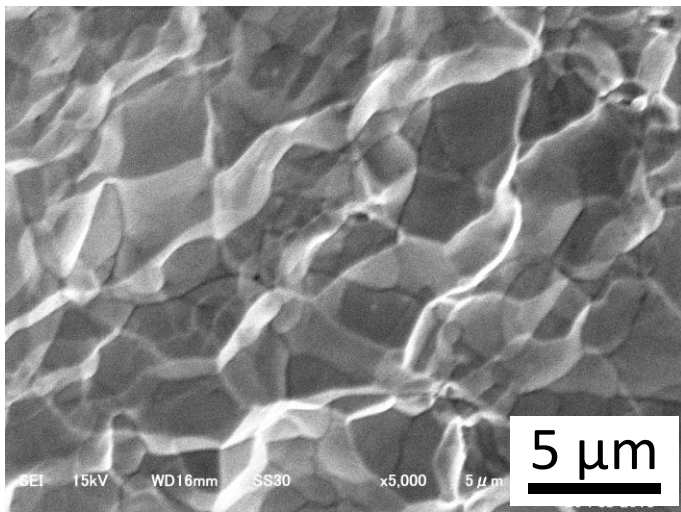
(c) K-doped W (7 mm) / 800 °C
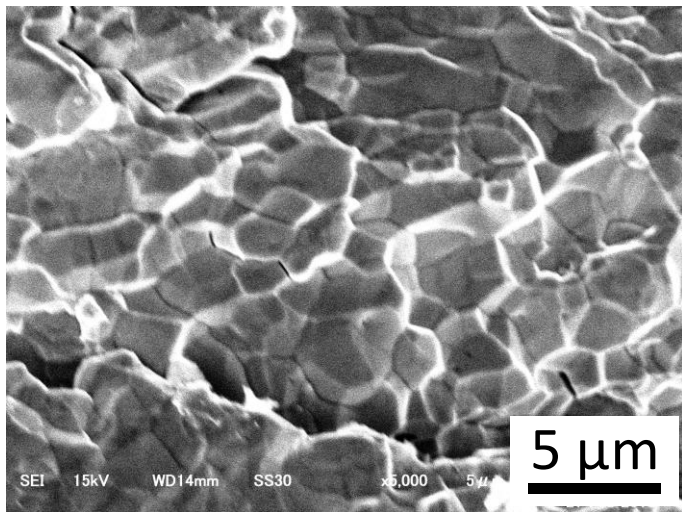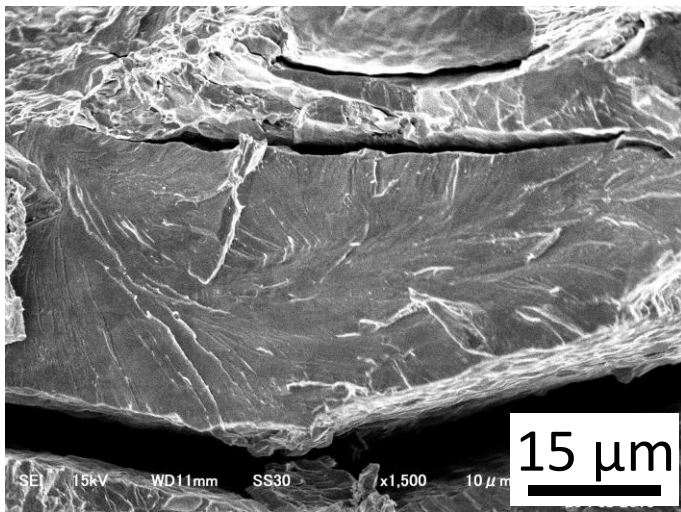
(b) Pure W (7 mm) / 400 °C

(d) K-doped W (7 mm) / 300 °C
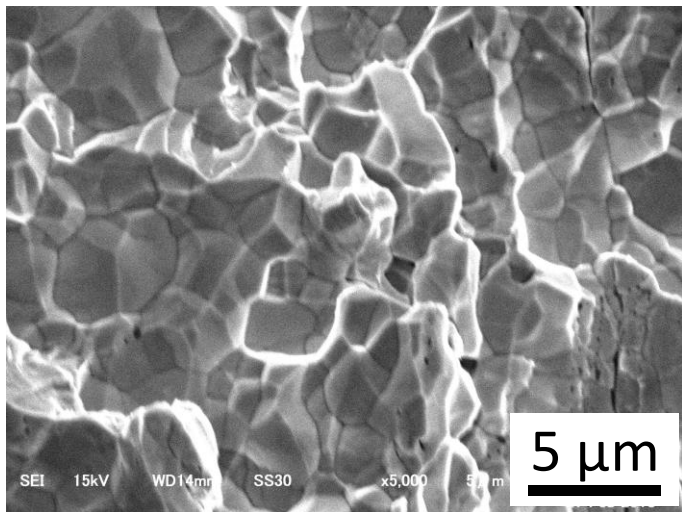
Fig. 9

(a) Pure W (7 mm) / R.T. / 10^{-3} s^{-1}
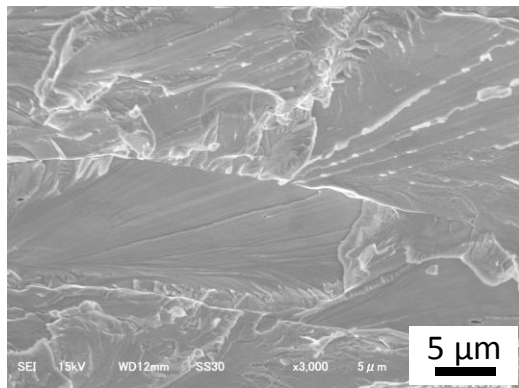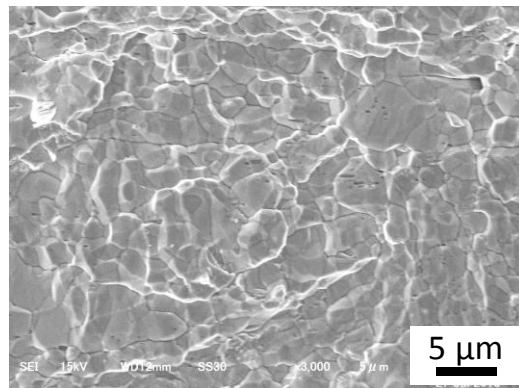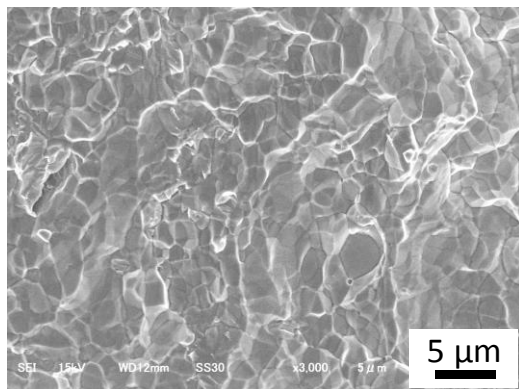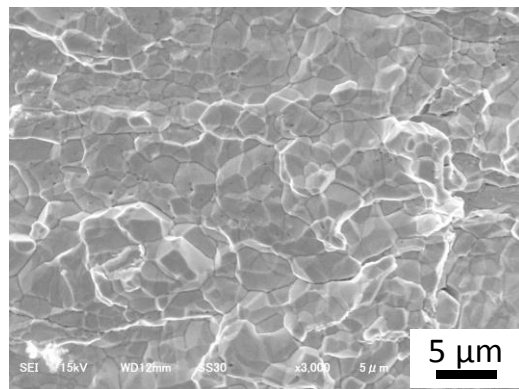
(e) K-doped W (7 mm) / R.T. / 10^{-3} s^{-1}

(b) Pure W (7 mm) / 700 °C / 10^{-3} s^{-1}
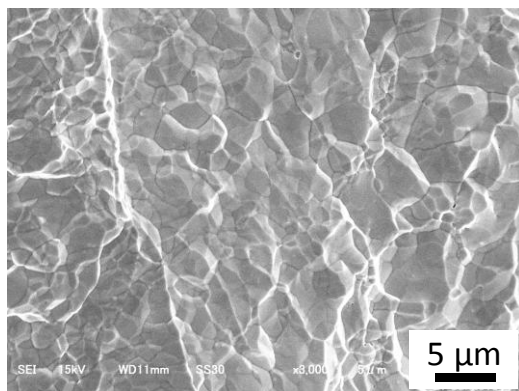

(f) K-doped W (7 mm) / 700 °C / 10^{-3} s^{-1}
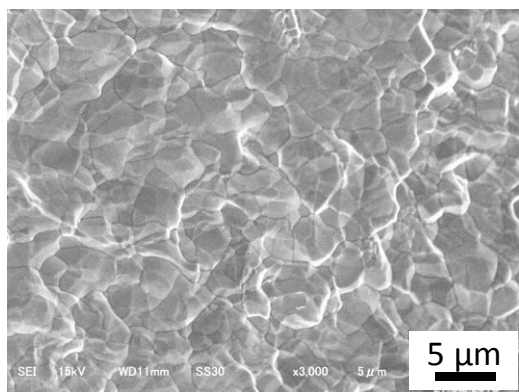
(c) Pure W (7 mm) / R.T. / 10^{-1} s^{-1}

(g) K-doped W (7 mm) / R.T. / 10^{-1} s^{-1}
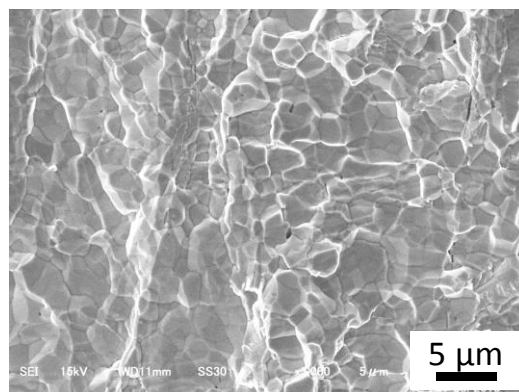
(d) Pure W (7 mm) / 700 °C / 10^{-1} s^{-1}

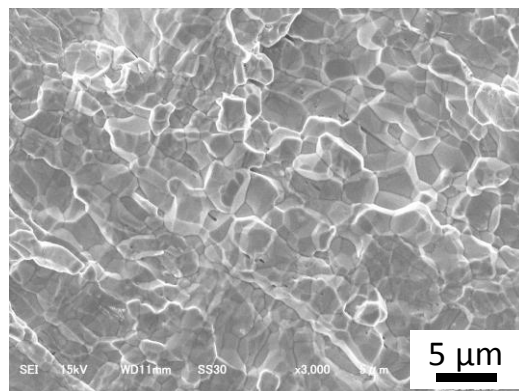
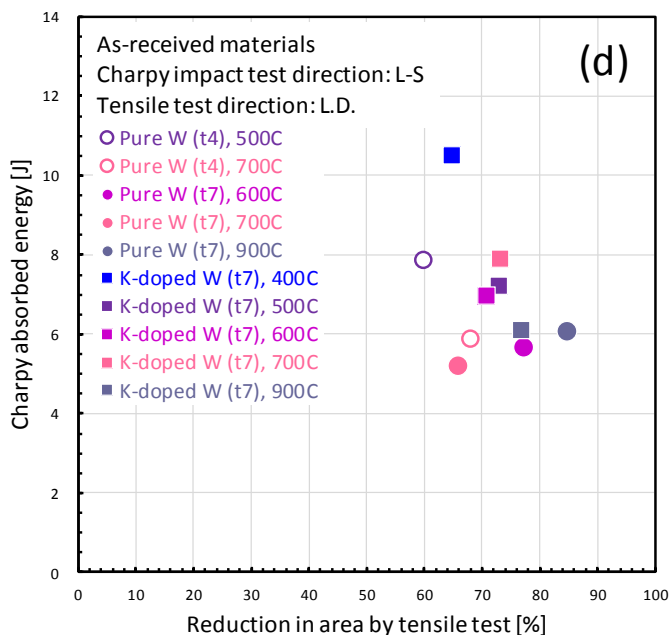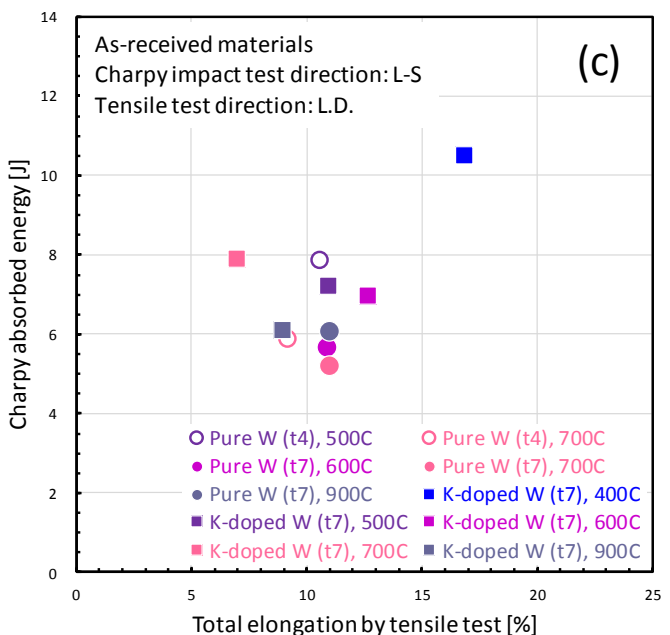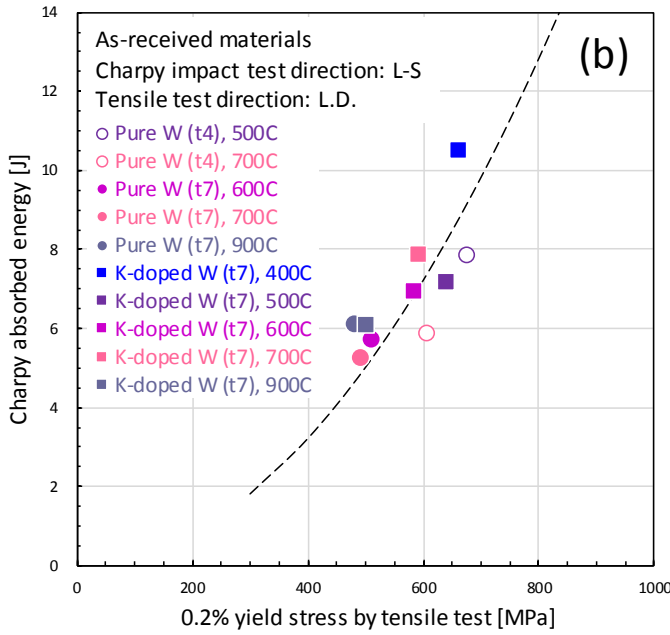(h) K-doped W (7 mm) / 700 °C / 10^{-1} s^{-1}

Fig. 10

Fig. 11

Fig. 12

	(a) Pure W (7 mm thick)		(b) K-doped W (7 mm thick)	
	IPF	KAM	IPF	KAM
As-Recieved				
1100 °C				
1200 °C				
1300 °C				
1400 °C				
1500 °C				
2300 °C				